

2016 Fall

“Phase Transformation *in* Materials”

12.07.2016

Eun Soo Park

Office: 33-313

Telephone: 880-7221

Email: espark@snu.ac.kr

Office hours: by an appointment

5.5.5 Spinodal Decomposition

Spinodal mode of transformation has no barrier to nucleation

: describing the transformation of a system of two or more components in a metastable phase into two stable phases

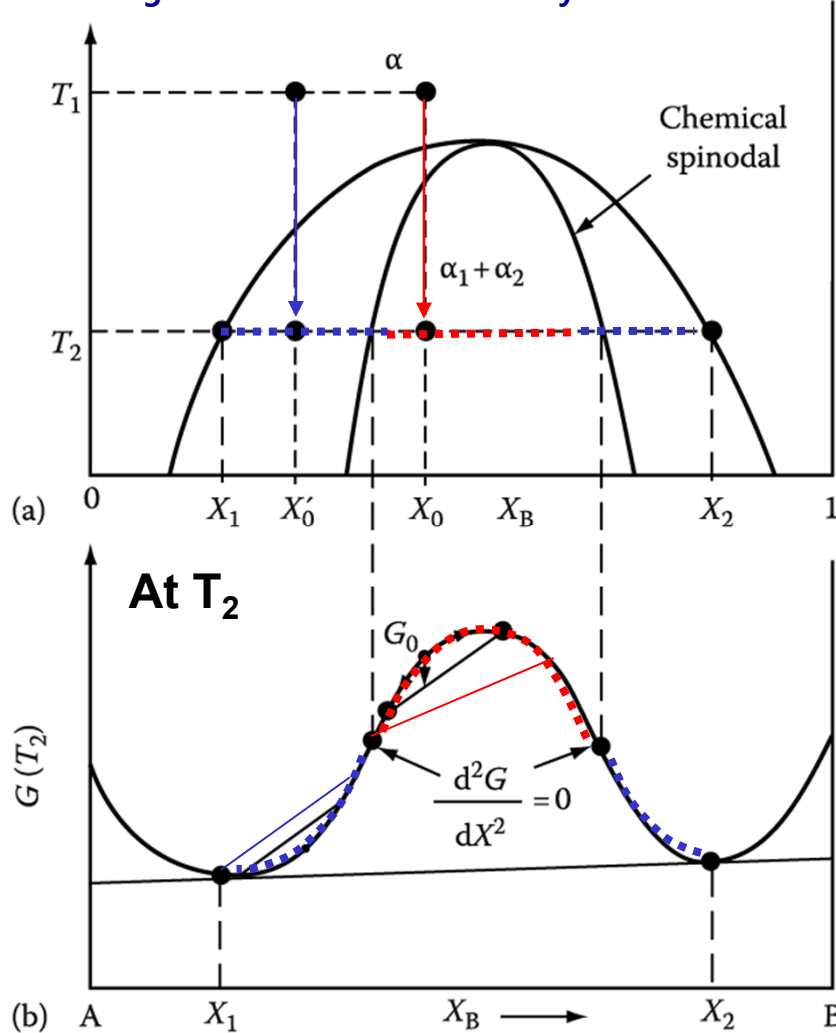


Fig. 5.38 Alloys between the spinodal points are unstable and can decompose into two coherent phases α_1 and α_2 without overcoming an activation energy barrier. Alloys between the coherent miscibility gaps and the spinodal are metastable and can decompose only after nucleation of the other phase.

How does it differ between **inside** and **outside the inflection point** of Gibbs free energy curve?

1) **Within the spinodal** $\frac{d^2G}{dX^2} < 0$

: phase separation by small fluctuations in composition/
"up-hill diffusion"

2) If the alloy lies **outside the spinodal**, small variation in composition leads to an increase in free energy and the alloy is therefore **metastable**.

The free energy can only be decreased if nuclei are formed with a composition very different from the matrix.

→ **nucleation and growth**
: "down-hill diffusion"

a) Composition fluctuations within the spinodal

b) Normal down-hill diffusion outside the spinodal

up-hill diffusion

down-hill diffusion

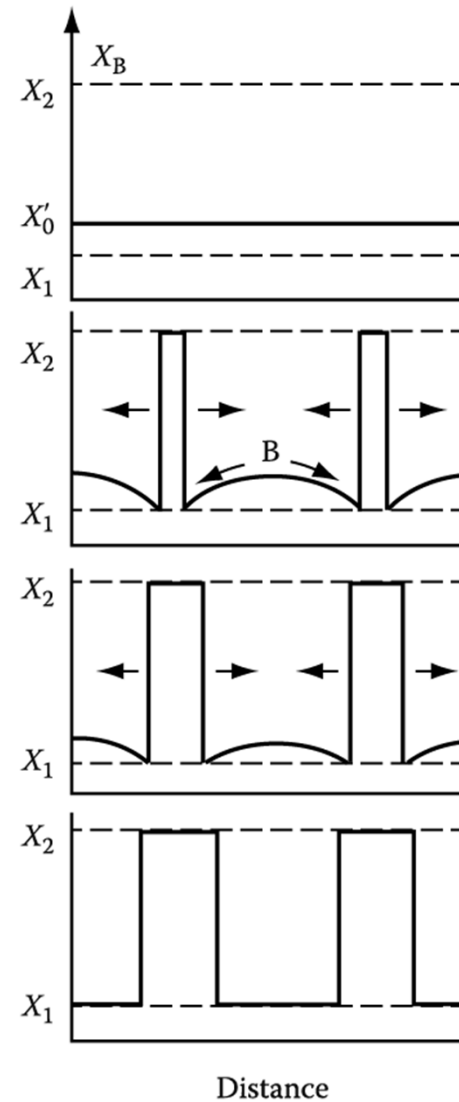
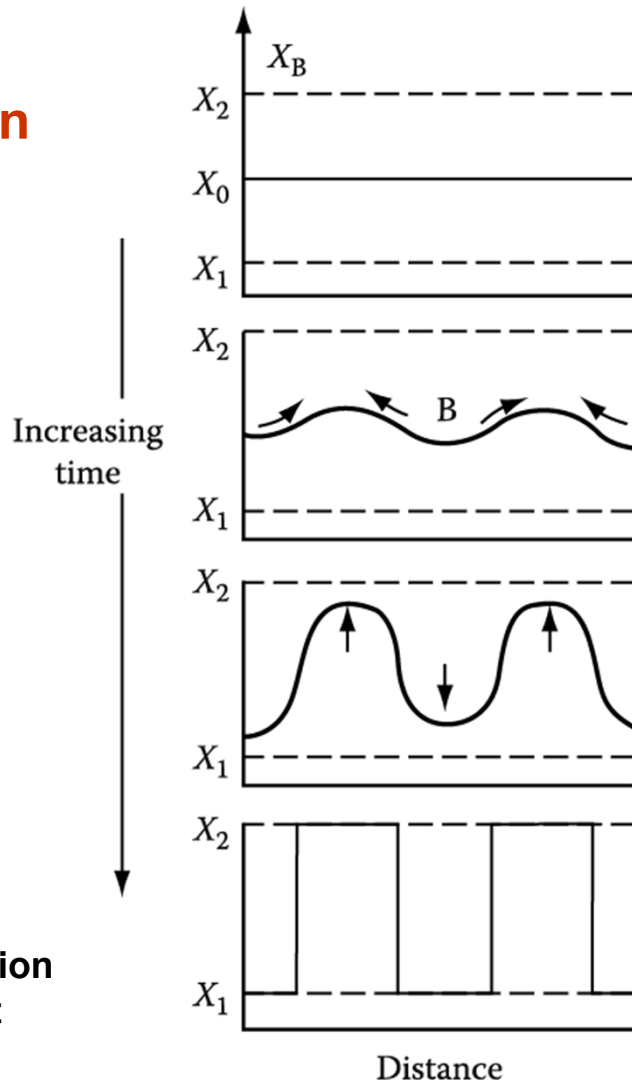


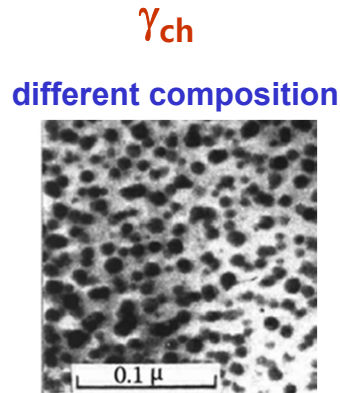
Fig. 5.39 & 5.40 schematic composition profiles at increasing times in (a) an alloy quenched into the spinodal region (X_0 in Figure 5.38) and (b) an alloy outside the spinodal points (X'_0 in Figure 5.38)

3.4 Interphase Interfaces in Solids

$$\sum A_i \gamma_i + \Delta G_S = \text{minimum}$$

Lowest total interfacial free energy
by optimizing the **shape of the precipitate** and **its orientation relationship**

Fully coherent precipitates



$\gamma_{ch} + \text{Lattice misfit}$ $\rightarrow \gamma_{ch} + \text{Volume Misfit } \Delta = \frac{\Delta V}{V}$

Coherency strain energy Chemical and structural interfacial E

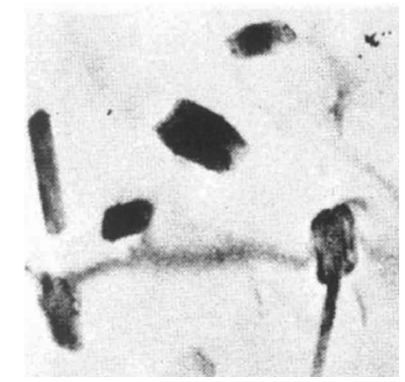
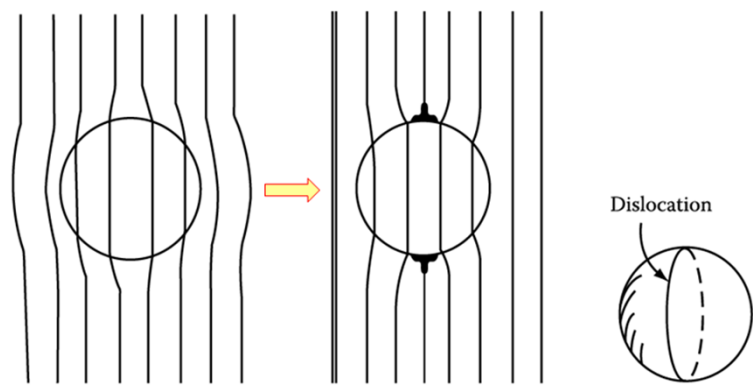
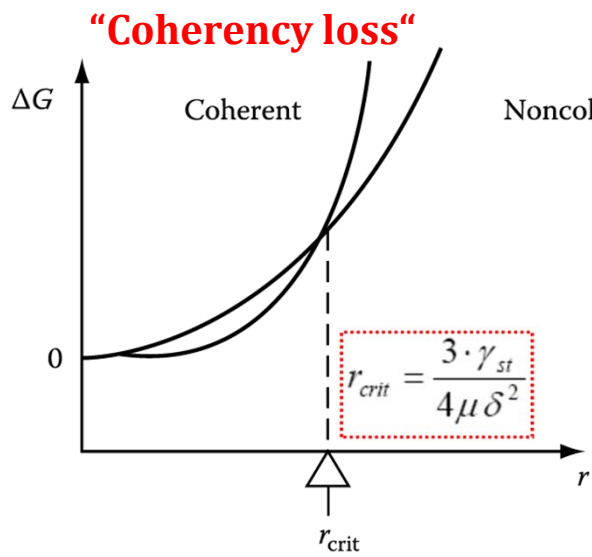
$\Delta G_S = 4\mu\delta^2 \cdot V$ (If $\nu=1/3$) $\leftrightarrow \Delta G_S = \frac{2}{3}\mu\Delta^2 \cdot V \cdot f(c/a)$

Fully coherent precipitates Incoherent inclusions

$$\Delta G(\text{coherent}) = 4\mu\delta^2 \cdot \frac{4}{3}\pi r^3 + 4\pi r^2 \cdot \gamma_{ch}$$

$\Delta G(\text{non-coherent}) = 4\pi r^2 \cdot (\gamma_{ch} + \gamma_{st})$

Incoherent inclusions



This figure include the lines defining the equilibrium compositions of the coherent/ incoherent phases that result from spinodal decomposition.

*** Incoherent(or equilibrium) miscibility gap: $\Delta H > 0$**

The miscibility gap the normally appears on an equilibrium phase is the incoherent (or equilibrium) miscibility gap. → equilibrium compositions of incoherent phases without strain fields.

a) chemical spinodal: $d^2G/dX^2=0$ _no practical importance X

b) Area ② , $\Delta G_V - \Delta G_S < 0$ → only incoherent strain-free nuclei can form.

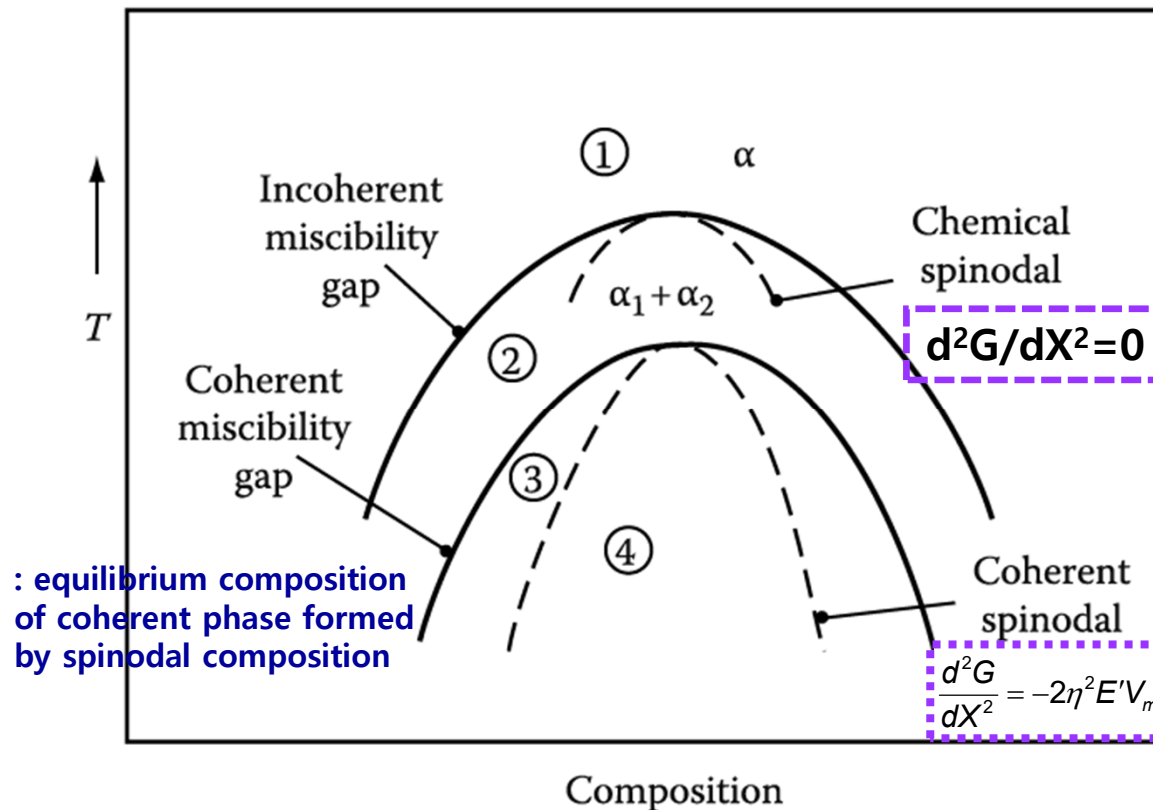


Figure 5.41 Schematic phase diagram for a clustering system.

Region 1: homogeneous α stable. Region 2: homogeneous α metastable, only incoherent phases can nucleate. Region 3: homogeneous α metastable, coherent phase can nucleate. Region 4: homogeneous α unstable, no nucleation barrier, spinodal decomposition occurs.

Spinodal decomposition is not only limited to systems containing a stable miscibility gap

All systems in which GP zones form, for example, containing a metastable coherent miscibility gap, i.e., the GP zone solvus.

→ at high supersaturation, GP zone can form by the spinodal mechanism.

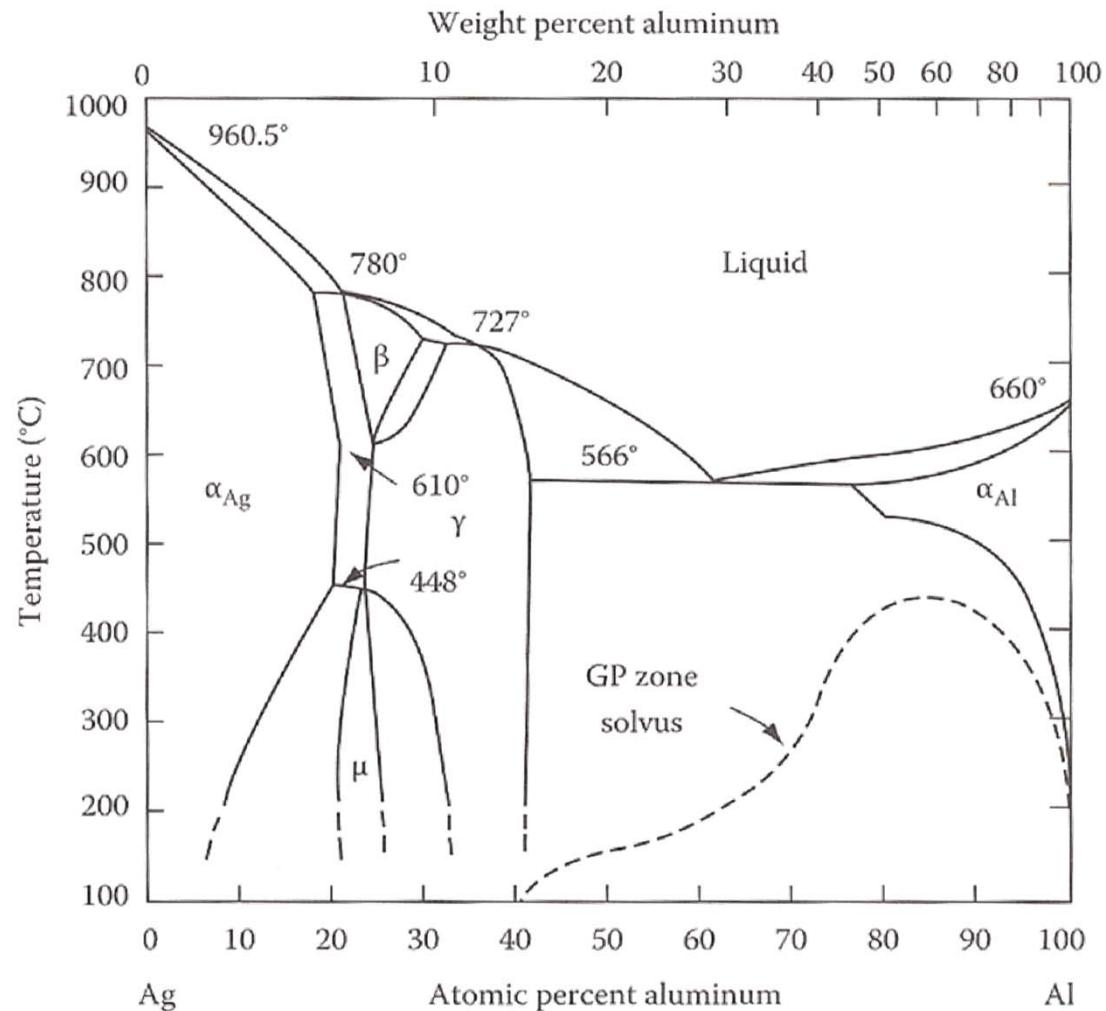


Figure 5.34

Al-Ag phase diagram showing metastable two-phase field corresponding to GP zones.

Microstructure of a two phase alloy is always unstable if the total interfacial free E is not a minimum. →

5.5.6. Particle Coarsening (smaller total interfacial area → loss of strength or disappearance of GB pinning effect → particular concern in the design of materials for high temp. applications)

Two Adjacent Spherical Precipitates with Different Diameters

(Gibbs-Thomson effect: radius of curvature ↓ → X_B ↑)

Assumption: volume diffusion is the rate controlling factor

$$(\bar{r})^3 - r_0^3 = kt$$

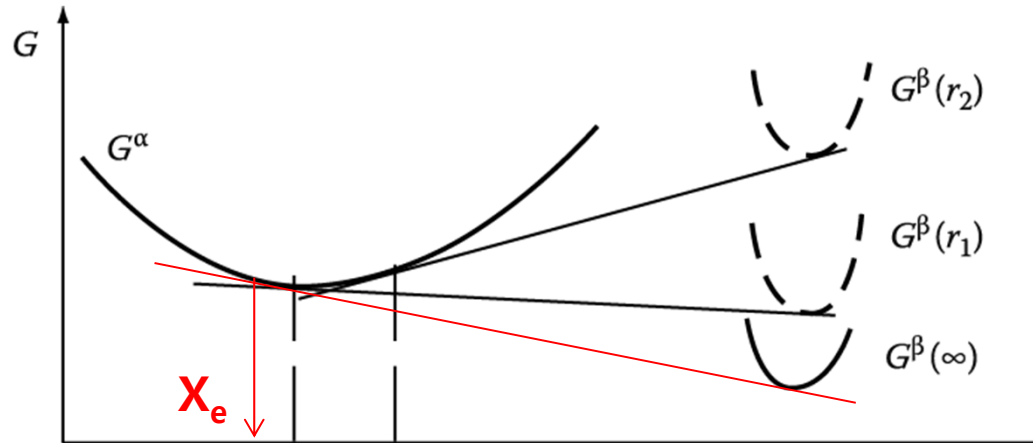
Average radius

where $k \propto D_\gamma X_e$

(X_e : Equil. solubility of very large particles)

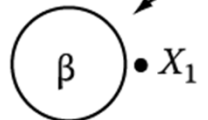
Coarsening rate

$$\frac{d\bar{r}}{dt} \propto \frac{k}{\bar{r}^2}$$

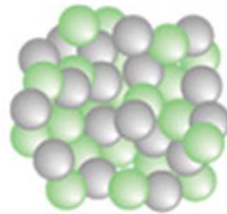


(b) $X_1 < X_2$ X_B →
A-rich B-rich

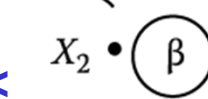
Lower density of larger particles



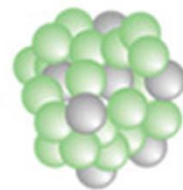
A-rich r_1



B



B-rich r_2

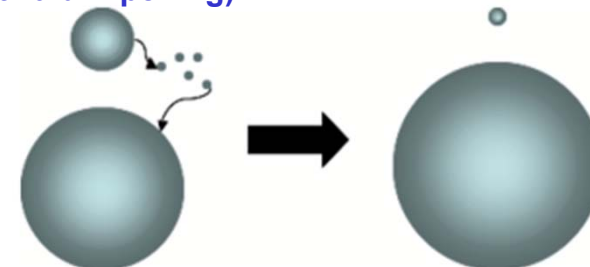


High density of small precipitates

(D and $X_e \sim \exp(-Q/RT)$)
 \bar{r} Rapidly increase with Increasing temp.

⇒ CR ↑

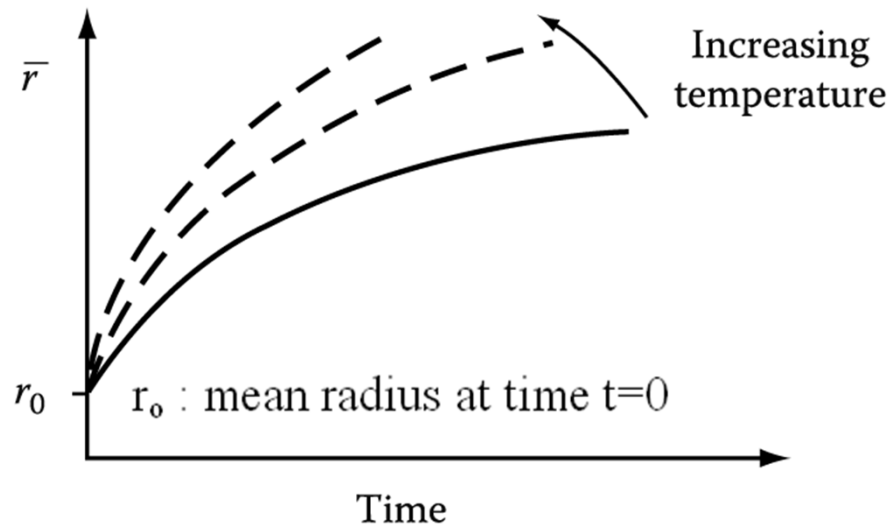
(Ostwald Ripening)



: Concentration gradient in matrix → diffusion → small particle_shrink/ large particle_grow

5.5.6. Particle Coarsening

The Rate of Coarsening with Increasing Time and Temp.



\bar{r} ~ Particular concern in the design of materials for high temperature applications

Undesirable degradation of properties:
less strength/ disappearance of GB pinning effects

How can you design an alloy with high strength at high T?

→ fine precipitate dispersion

hint) $\frac{d\bar{r}}{dt} \propto \frac{k}{\bar{r}^2}$ $k \propto D\gamma X_e$

1) low γ

heat-resistant Nimonic alloys

based on Ni-rich Ni-Cr → ordered fcc

$\text{Ni}_3(\text{Ti,Al})$ in Ni-rich matrix → high strength

Ni/ γ' interface ~ “fully coherent” (10 ~ 30 mJ m⁻²)

Maintain a fine structure at high temperature

→ improve creep-rupture life

2) low X_e (Oxide ~ very insoluble in metals)

: fine oxide dispersion in a metal matrix

Ex) dispersed fine ThO_2 (thoria) in W and Ni

→ strengthened for high temperature

3) low D

Cementite dispersions in tempered steel

→ high D of carbon → very quickly coarsening

a. substitutional alloying element

→ segregates to carbide → slow coarsening

b. strong carbide-forming elements

→ more stable carbides → lower X_e

5.6. The Precipitation of Ferrite from Austenite

Typical TTT curve for $\gamma \rightarrow \alpha$ transformation $\rightarrow f(t, T)$

J-M-A Eq.

$$f = 1 - \exp(-kt^n)$$

k : sensitive with T $f(I, v) \sim \frac{\pi}{3} I v^3$
 n : 1 ~ 4 (depend on nucleation mechanism)

- a) Time for a given percentage transformation will decrease as the constant k increase
 - b) k increases with increases in ΔT or total # of nucleation sites
- \rightarrow Thus, decreasing the austenite grain size has the effect of shifting the C curve to shorter transformation times.

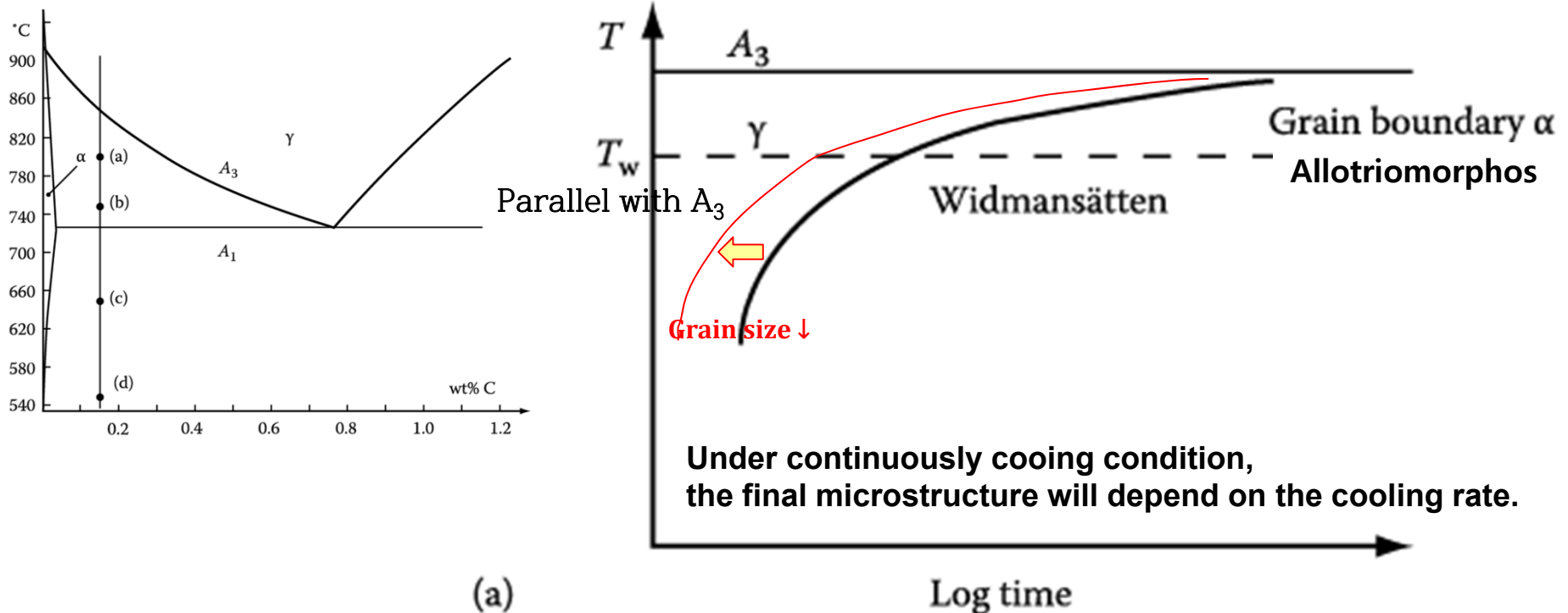
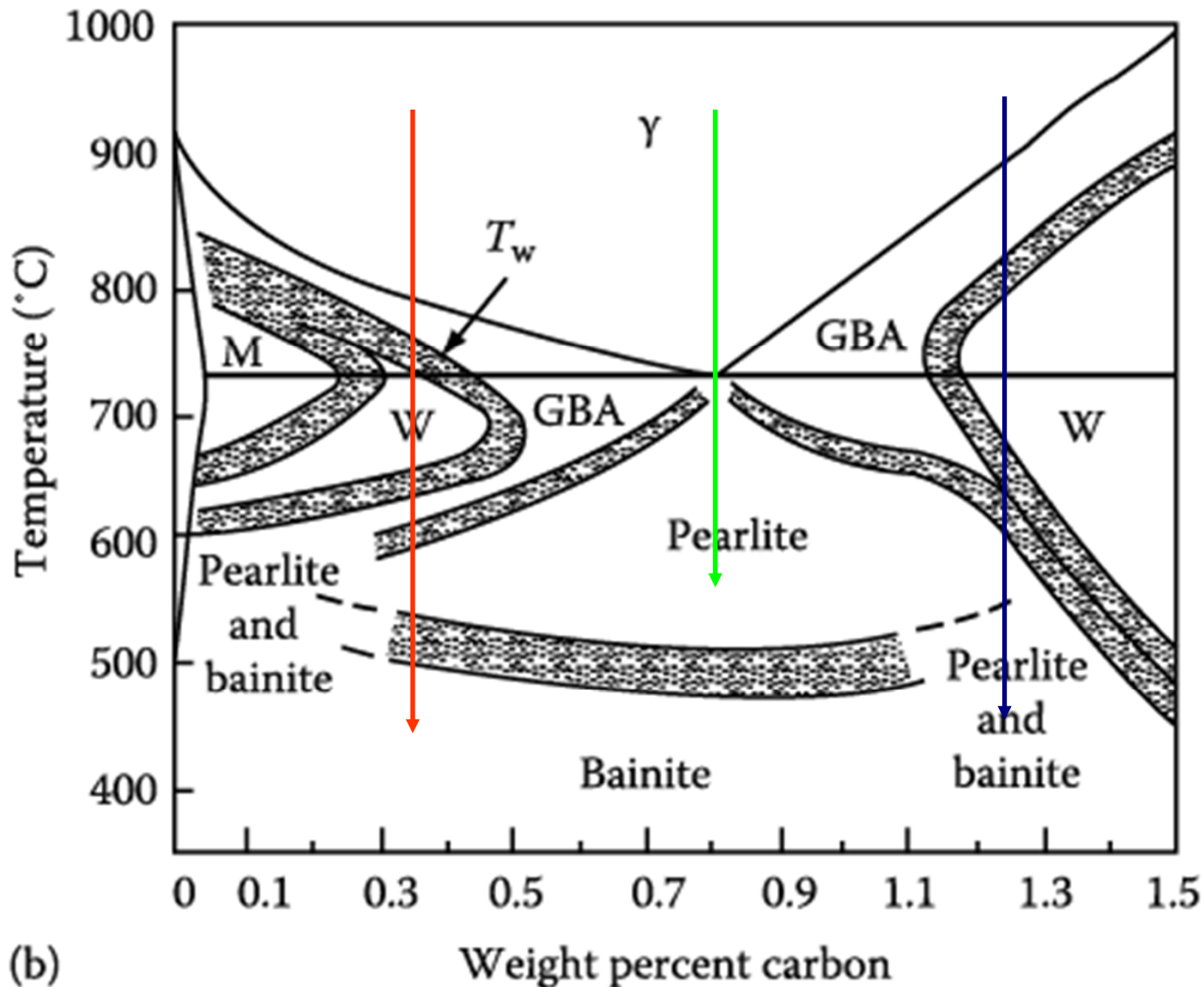


Figure 5.48 (a) typical TTT curve for $\gamma \rightarrow \alpha$ transformation in a hypoeutectoid steel: a typical C shape.

For alloys of different carbon content, A_3 and T_w vary and show parallel manner each other.



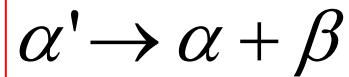
(GBA: GB allotriomorphs, W: Widmanstätten sideplates/intermolecular plates, M: Massive ferrite)

Figure 5.48 (b) Temperature-composition regions in which the various morphologies are dominant at late reaction times in specimens with ASTM grain size Nos. 0-1. 10

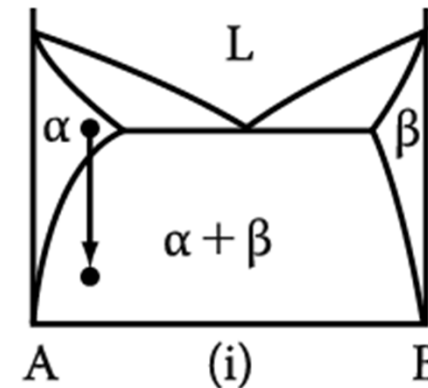
5. Diffusion Transformations in solid

: diffusional nucleation & growth

(a) Precipitation



Metastable supersaturated
Solid solution



Homogeneous Nucleation

$$\Delta G = -V\Delta G_V + A\gamma + V\Delta G_S$$

Heterogeneous Nucleation

$$\Delta G_{het} = -V(\Delta G_V - \Delta G_S) + A\gamma - \Delta G_d$$

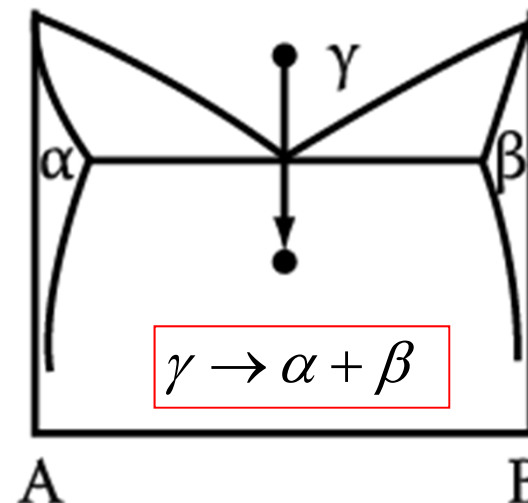
$$N_{hom} = \omega C_0 \exp\left(-\frac{\Delta G_m}{kT}\right) \exp\left(-\frac{\Delta G^*}{kT}\right)$$

→ suitable nucleation sites ~ nonequilibrium defects
(creation of nucleus ~ destruction of a defect (-ΔG_d))

(b) Eutectoid Transformation

Composition of product phases
differs from that of a parent phase.

→ long-range diffusion



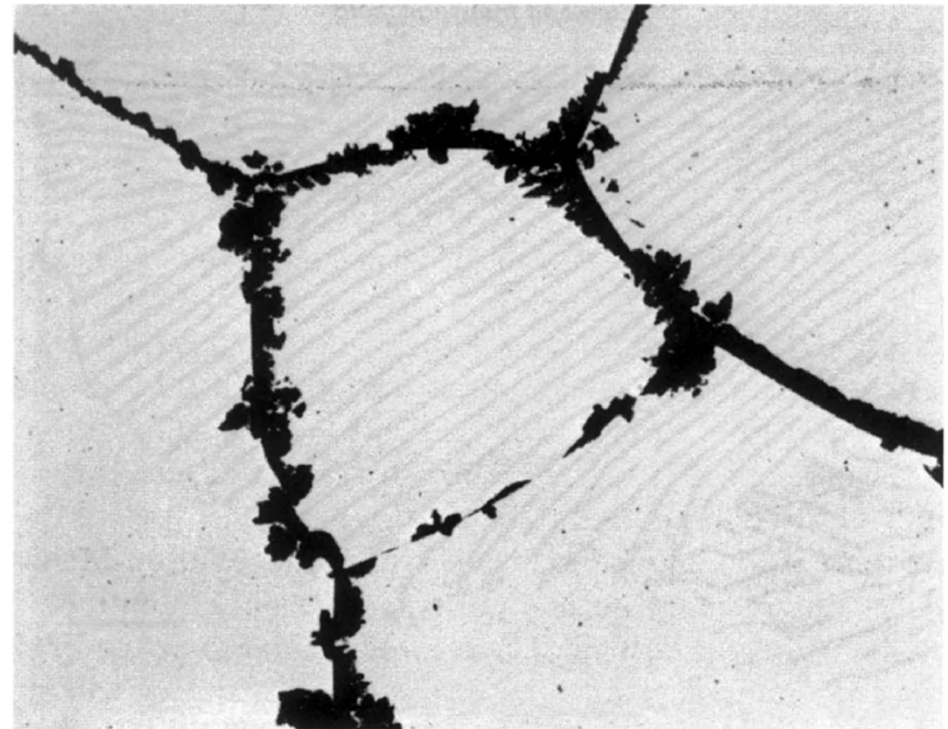
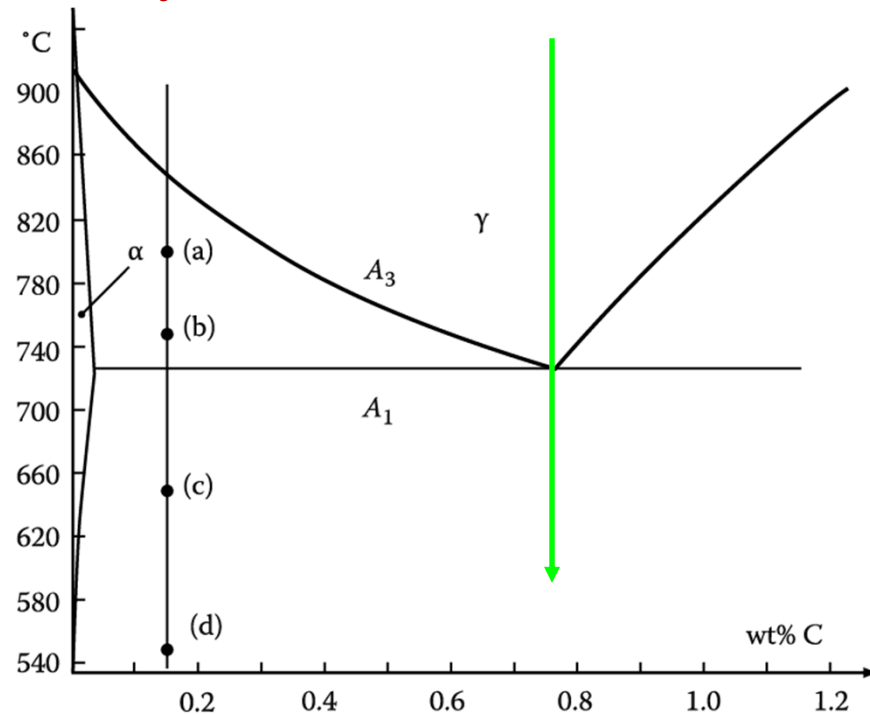
5.8. Eutectoid Transformation

5.8.1 Pearlite Reaction in Fe-C Alloys



Pearlite nodule nucleate on GBs and grow with a roughly constant radial velocity into the surrounding austenite grains.

Very similar to a eutectic transformation



* **At large undercooling,**

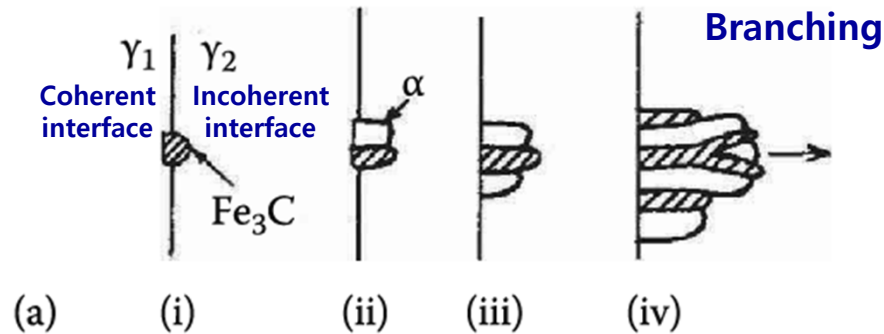
: the nucleation rate is much higher and site saturation occurs, that is all GBs become quickly covered with nodules which grow together forming layers of pearlite, Figure 5.61.

* **At small undercooling below A₁,**

: the number of pearlite nodules that nucleate is relatively small, and the nodules can grow as hemispheres or spheres without interfering with each other.

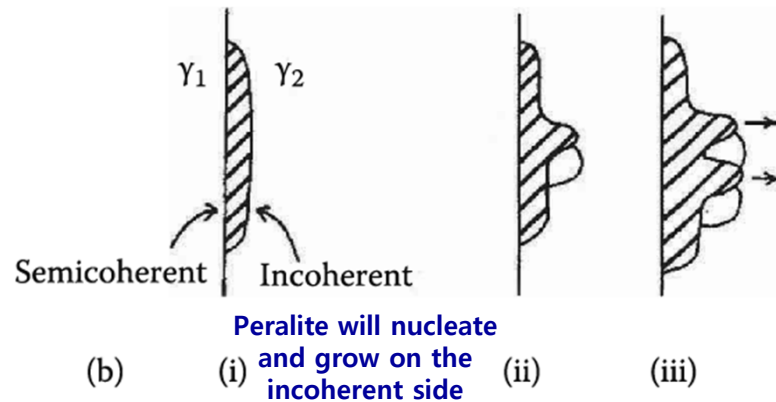
Pearlite Reaction in Fe-C Alloys: nucleation and growth

Nucleation: depend on **GB structures and composition**

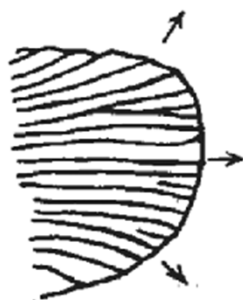


(a) On a “clean” GB.

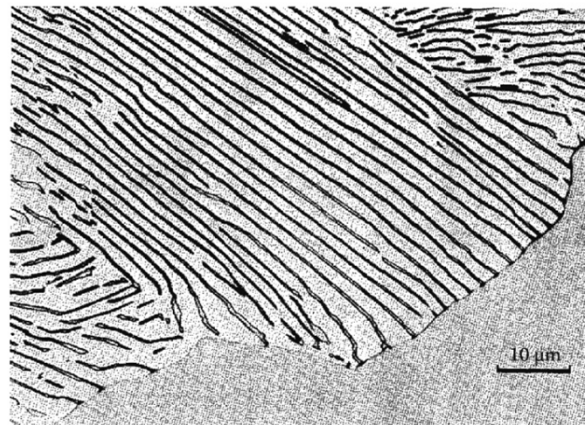
- (i) **Cementite nucleates on GB** with coherent interface and orientation relationship with γ_1 and incoherent interface with γ_2 .
- (ii) **α nucleates adjacent to cementite** also with a coherent interface and orientation relationship with γ_1 . (This also produces an orientation relationship between the cementite and the ferrite).
- (iii) The **nucleation process repeats side ways**, while incoherent interfaces grow into γ_2 .
- (iv) New plates can also form by a **branching mechanism**.



- (b) When a proeutectoid phase (cementite or ferrite) already exists on that boundary, pearlite will **nucleate and grow on the incoherent side**. A different orientation relationship between the cementite and the ferrite results in this case.



(c) A pearlite colony at a later stage of growth



- (c) **Pearlite colony** at a latest stage of growth. Pearlite grows into the austenite grain with which it does not have an orientation relationship.

Growth of Pearlite: analogous to the growth of a lamellar eutectic

Min. possible: $(S^*) \propto 1/\Delta T$ / Growth rate : mainly lattice diffusion $v = kD_c \gamma (\Delta T)^2$

Interlamellar spacing of pearlite colonies : mainly boundary diffusion $v = kD_b (\Delta T)^3$

Relative Positions of the Transformation curves for Pearlite and Bainite in Plain Carbon Eutectoid Steels.

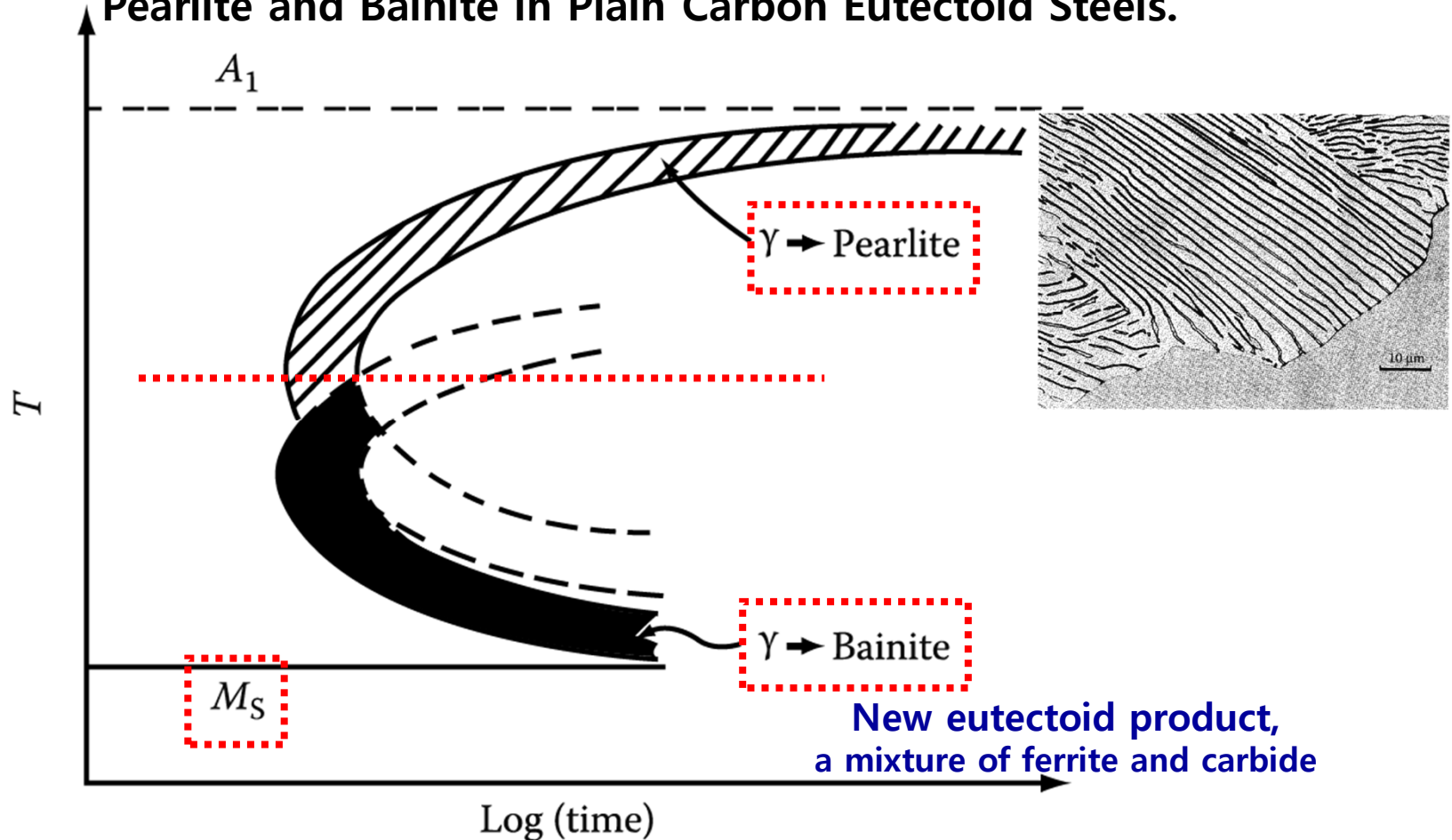


Figure 5.64 Schematic diagram showing relative positions of the transformation curves for pearlite and bainite in plain carbon eutectoid steel.

5.8.2 Bainite Transformation

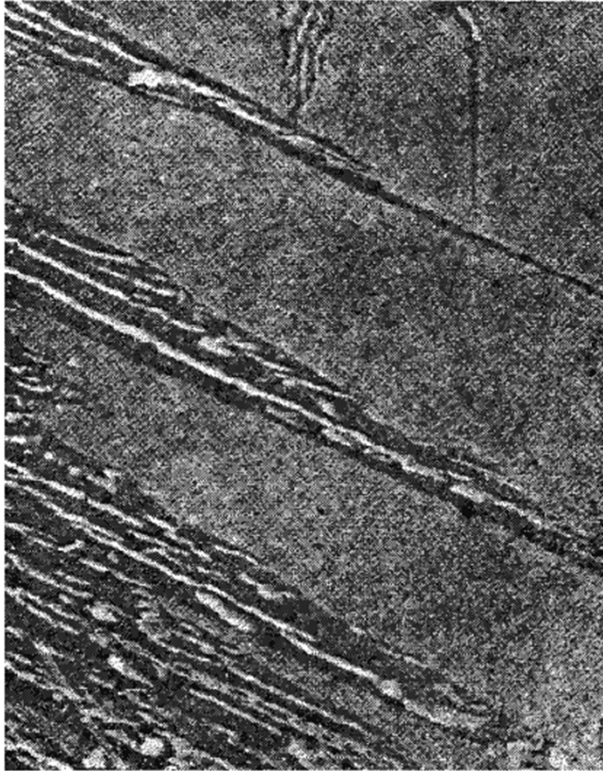
The microstructure of bainite depends mainly on the temperature at which it forms.

Upper Banite in medium-carbon steel

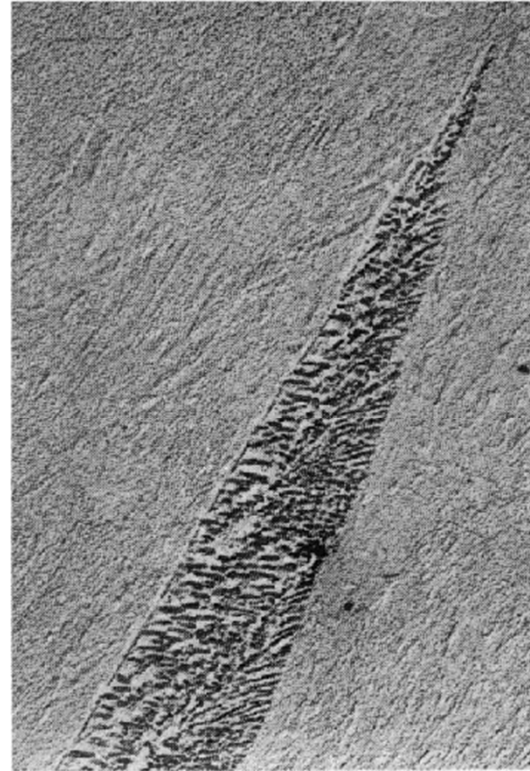
Lower Bainite in 0.69wt% C low-alloy steel

At high temp. 350 ~ 550°C, ferrite laths, K-S relationship, similar to Widmanstätten plates

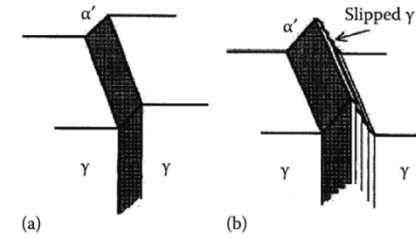
At sufficiently low temp. laths → plates
Carbide dispersion becomes much finer, rather like in tempered M.



(a)

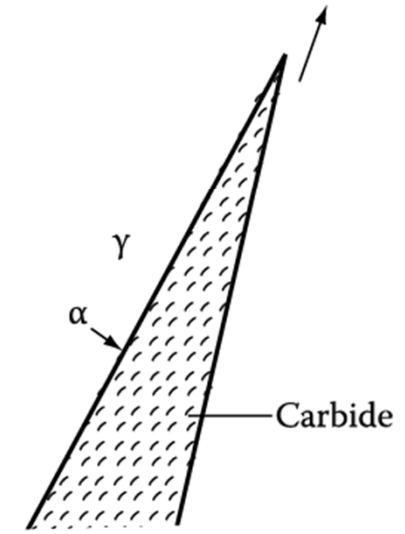


(a)

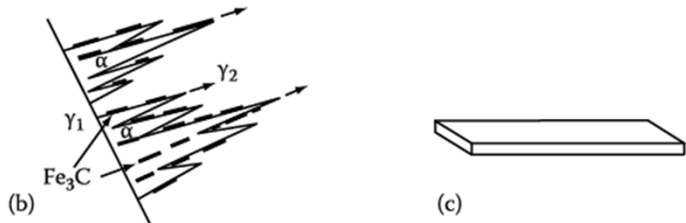


(a)

(b)



(b)



(b)

(c)

(b) Schematic of growth mechanism. Widmanstätten ferrite laths grow into γ_2 . Cementite plates nucleate in carbon-enriched austenite.

Surface tilts by bainite trans. like M trans.
Due to Shear mechanism/ordered military manner

(b) A possible growth mechanism. α/γ interface advances as fast as carbides precipitate at interface thereby removing the excess carbon in front of the α .

At the highest temp. where pearlite and bainite grow competitively.

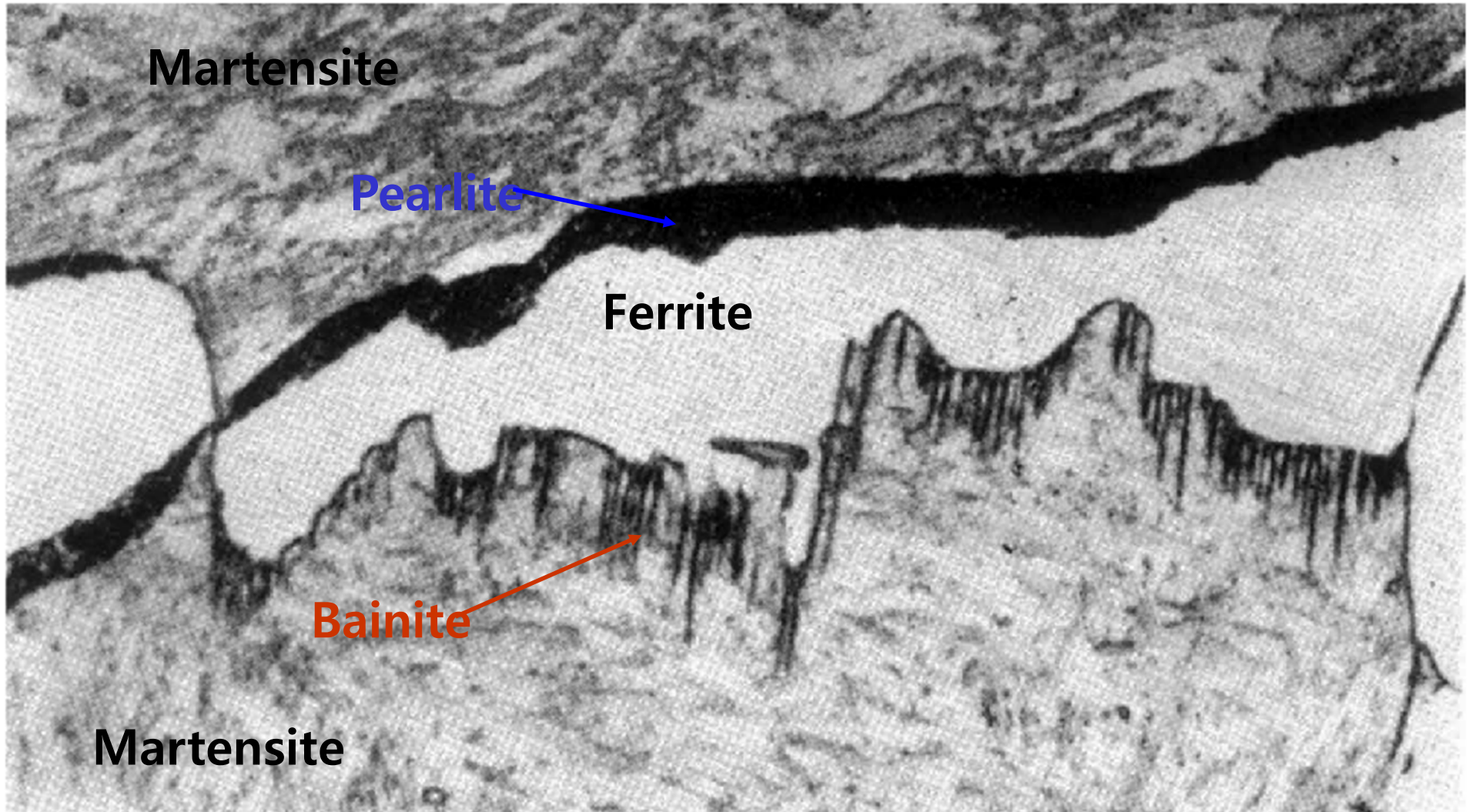


Fig. 5.67 Hypoeutectoid steel (0.6% C) partially transformed for 30 min at 710 °C. Inefficiently quenched. Bainitic growth into lower grain of austenite and pearlitic growth into upper grain during quench (x1800).

Pearlite : no specific orientation relationship

Bainite : orientation relationship

5.8.3 The effect of alloying elements on hardenability

: adding alloying elements to steels → delay to time required for the decomposition into ferrite and pearlite → M trans under slower cooling rate → increase hardenability

- * **Main factor limiting hardenability is the rate of formation of pearlite at the nose of the C curve in the TTT diagram.**
- Austenite stabilizer (Mn, Cu, Ni) – depress A3 temperature
- Ferrite stabilizer (Cr, Mo, Si) – increase A3 temperature

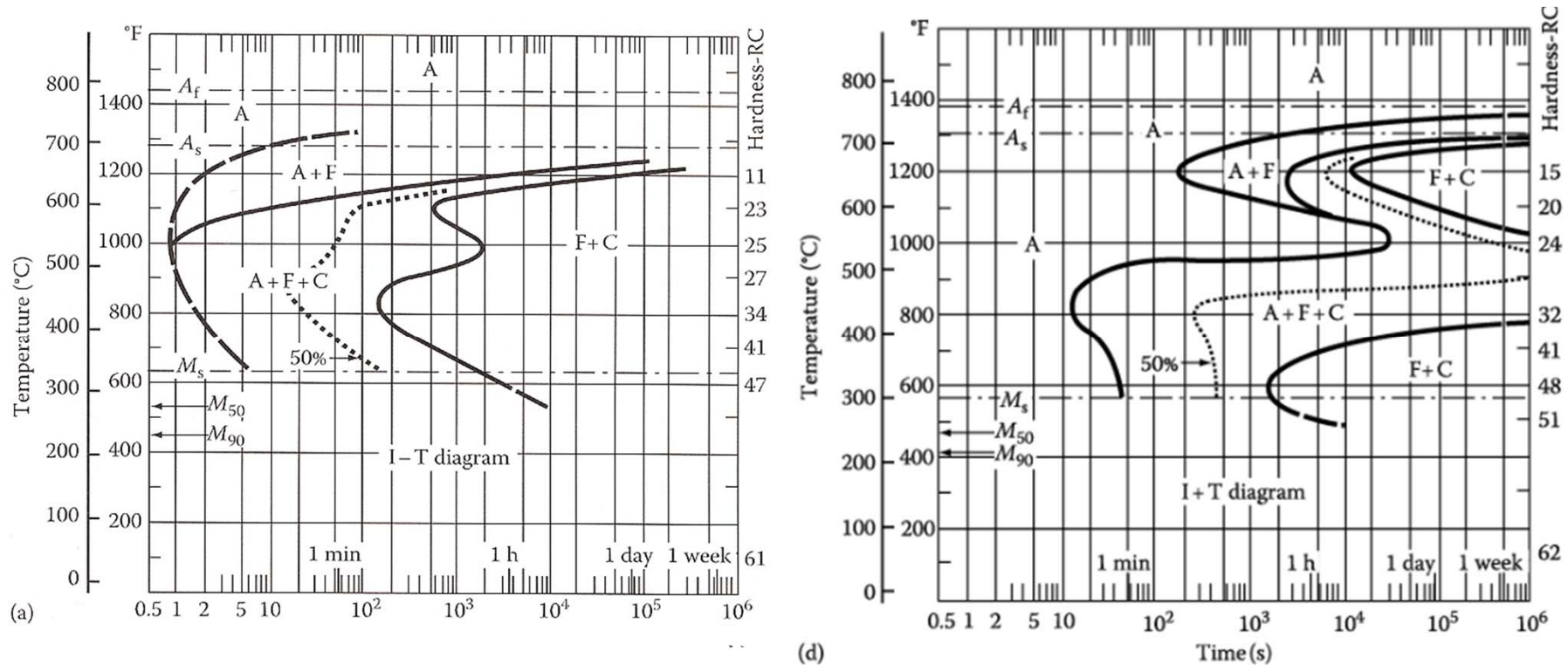
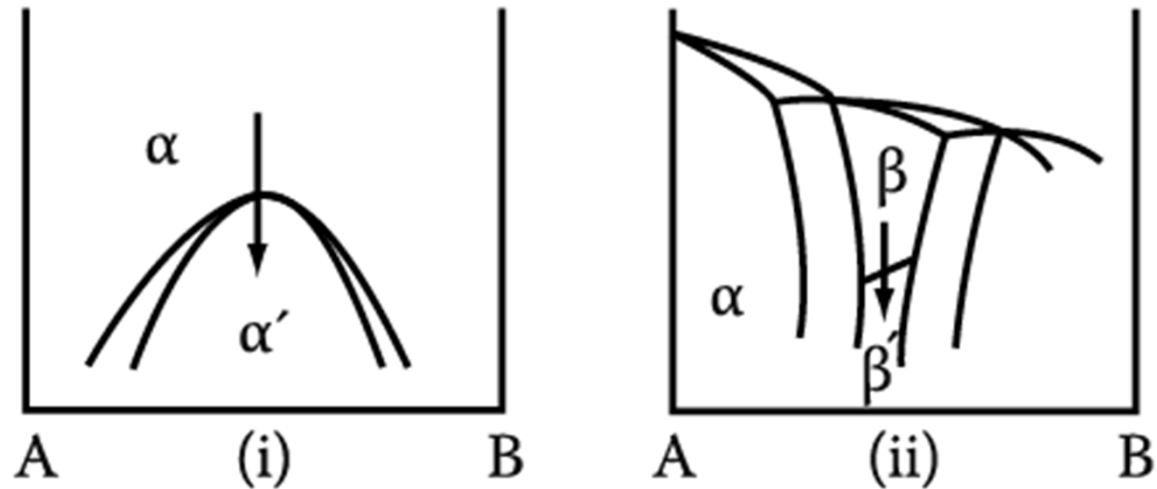
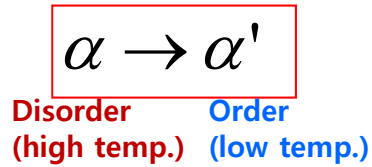


Figure 5.73 TTT diagrams for two commercial low-alloy steels all of which (a) contain roughly 0.4% C and 1% Mn and (b) contains 0.8% Cr, 0.3% Mo, and 1.8% Ni

5.8.4 - 5.8.6 skip

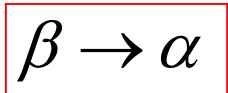
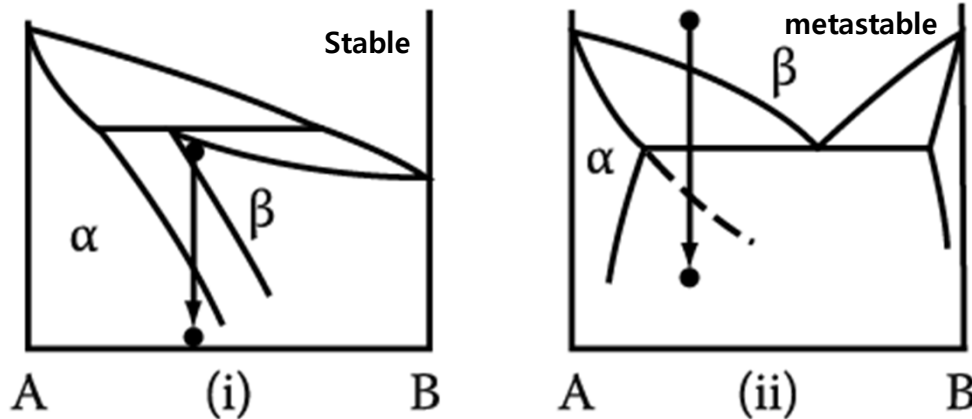
5. Diffusion Transformations in solid

(c) Order-Disorder Transformation

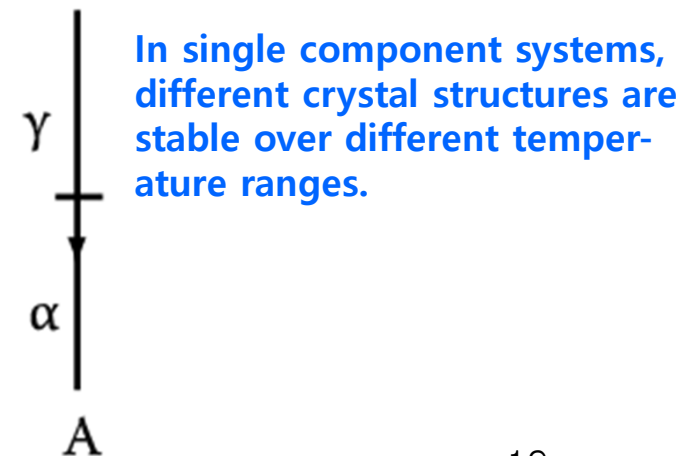


(d) Massive Transformation

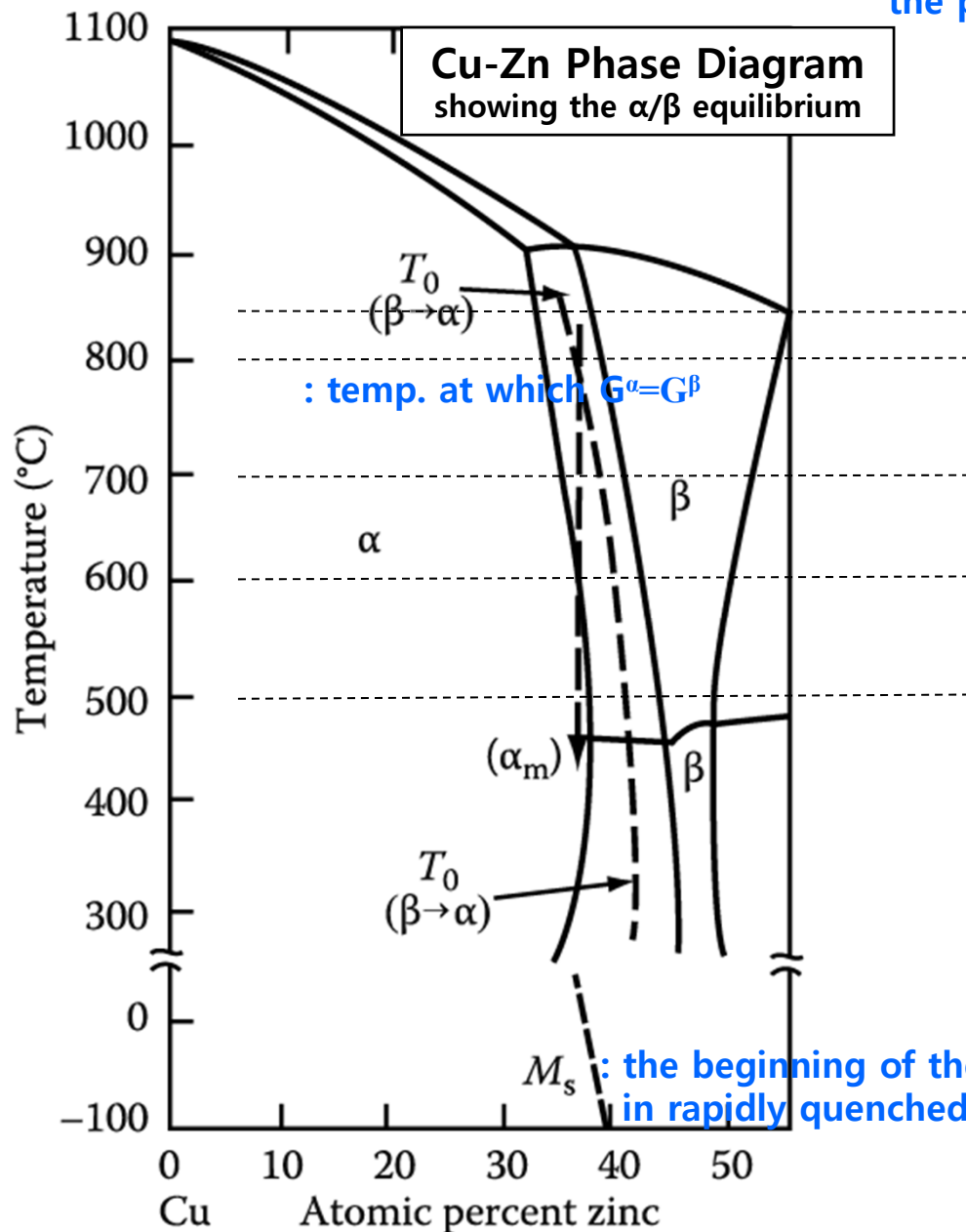
: The original phase decomposes into one or more new phases which have the same composition as the parent phase, but different crystal structures.



(e) Polymorphic Transformation

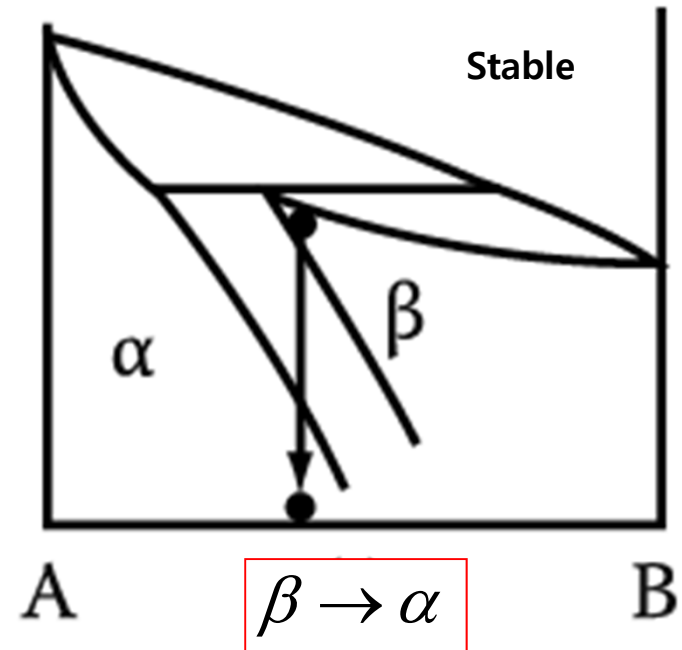


5.9 Massive Transformation : The original phase decomposes into one or more new phases which have the same composition as the parent phase, but different crystal structures.



: temp. at which $G^{\alpha}=G^{\beta}$

: the beginning of the M transformation in rapidly quenched specimens.



Free energy-composition curves for α and β at 850 $^{\circ}\text{C}$, 800 $^{\circ}\text{C}$, 700 $^{\circ}\text{C}$ and 600 $^{\circ}\text{C}$?

5.9 Massive Transformation

Free energy-composition curves for α and β

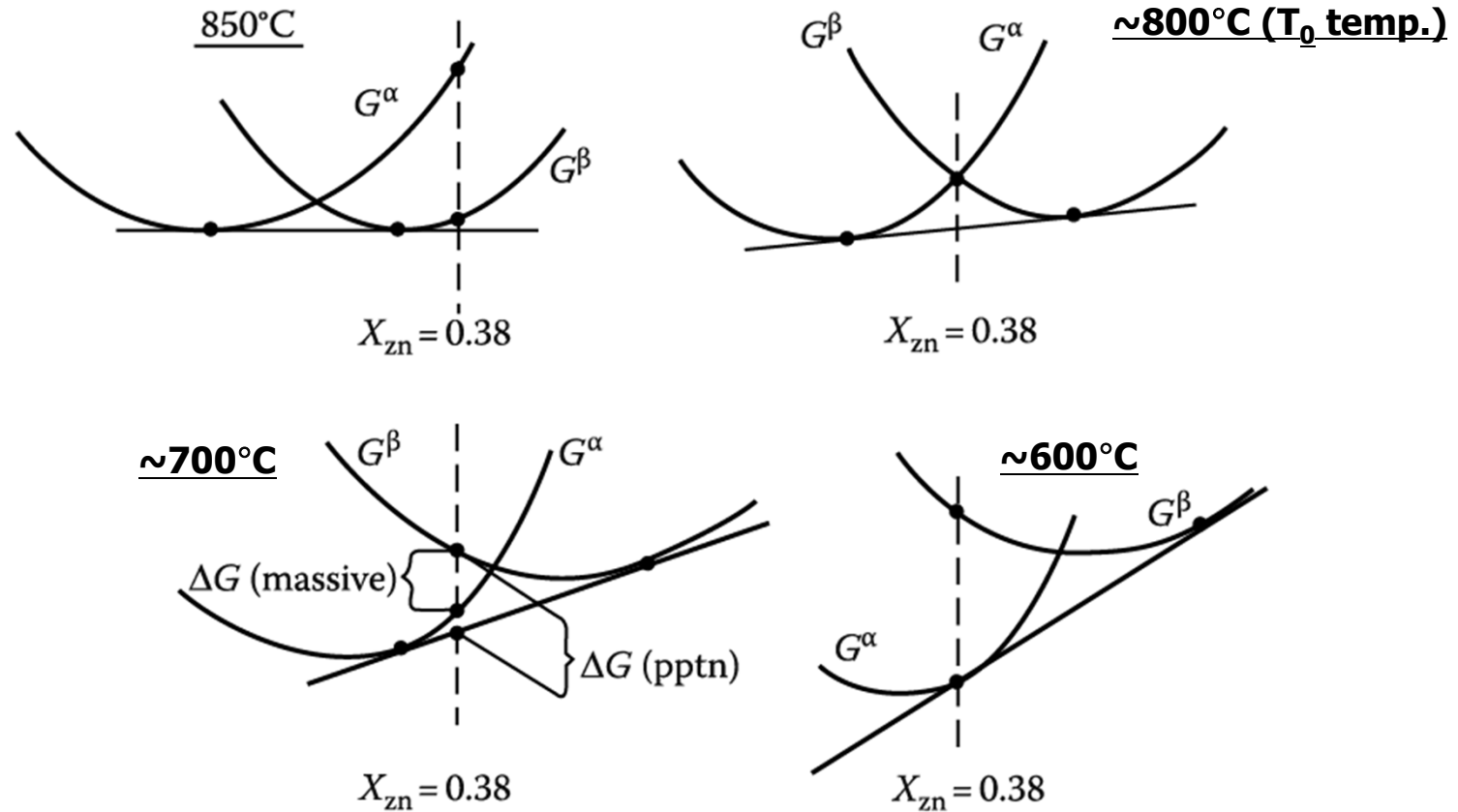


Fig. 5.86 A schematic representation of the free energy-composition curves for α and β in the Cu-Zn system at various temperatures.

At the thermodynamic point of view, it may possible for a massive trans. to occur within the two-phase region of the phase dia. anywhere below the T_0 temp.. But, in practice, there is evidence that massive trans. usually occur only within the single-phase region of the phase diagram

5.9 Massive Transformation

Massive α formed at the GBs of β and grow rapidly into the surrounding β

: a diffusionless civilian transformation (change of crystal structure without a change of composition)

Migration of the α/β interfaces~ very similar to the migration of GBs during recrystallization of single-phase material but, driving force ~ orders of magnitude greater than for recrystallization→ rapid growth: a characteristic irregular appearance.

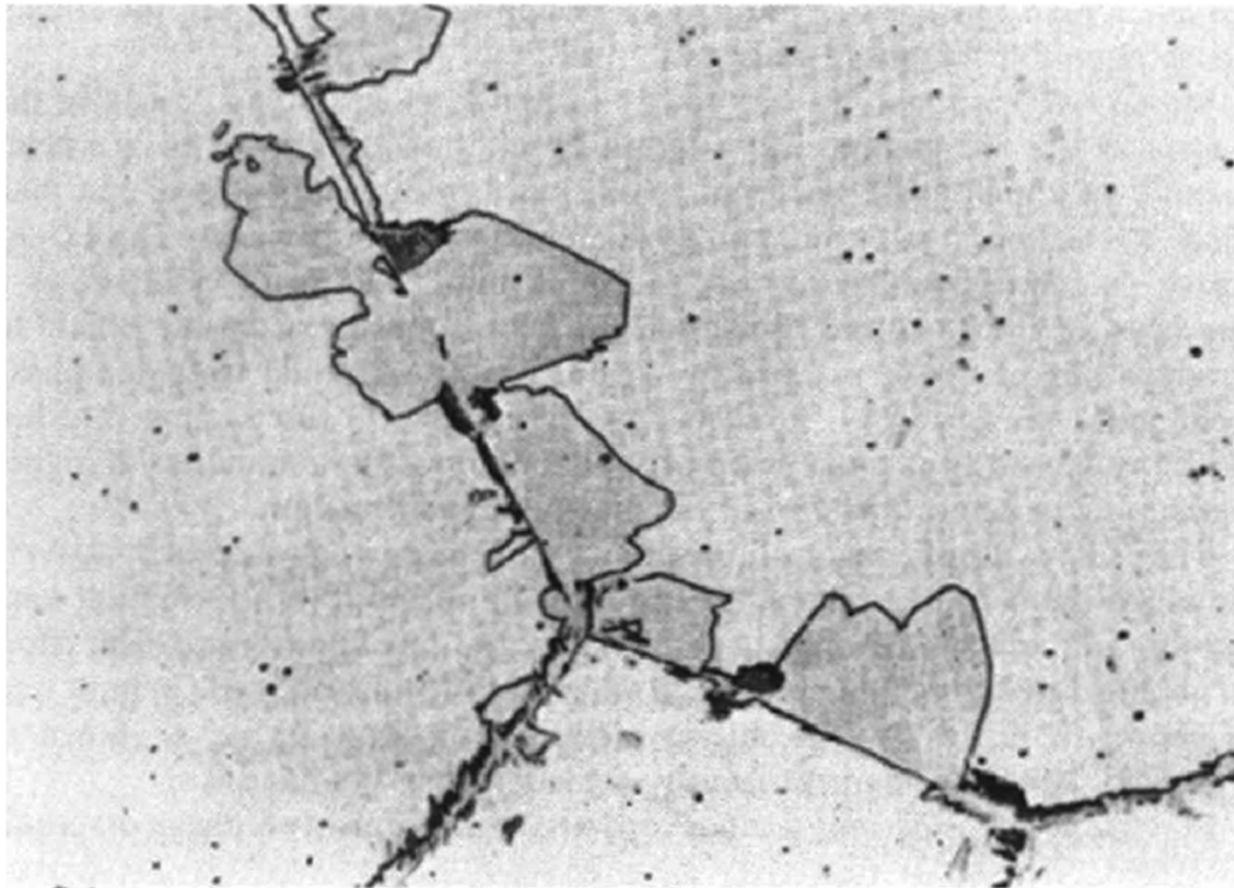
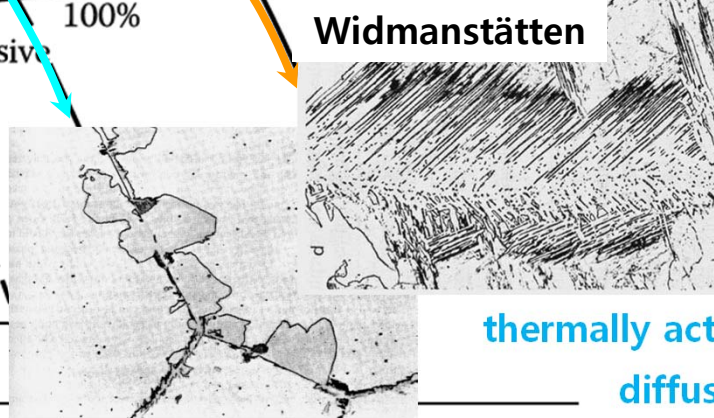
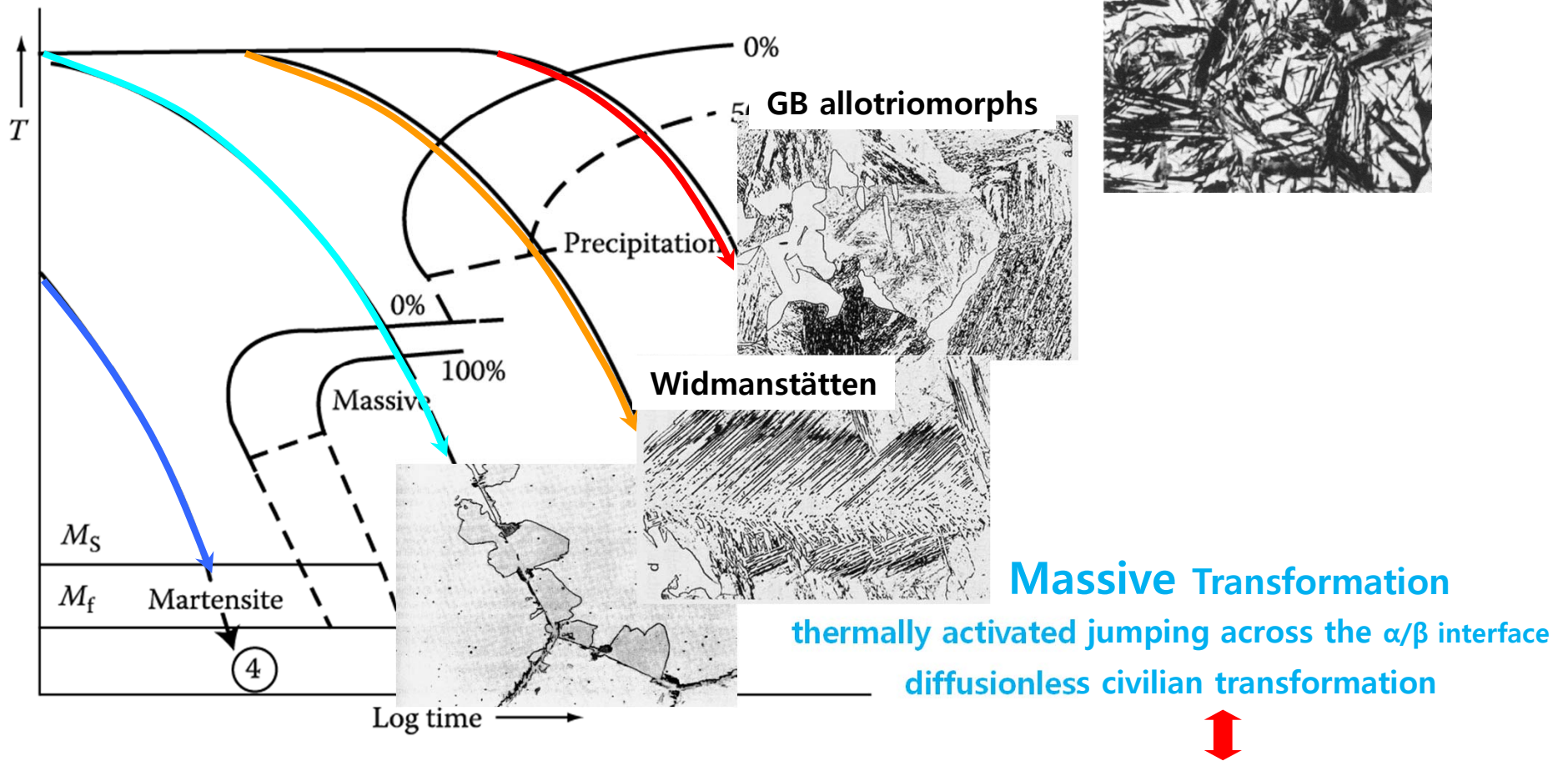


Figure 5.85 Massive α formed at the GBs of β in Cu-38.7wt% Zn quenched from 850 °C in brine at 0 °C. Some high temperature precipitation has also occurred on the boundaries.

* Massive, Martensite Transformation



Massive Transformation
 thermally activated jumping across the α/β interface
 diffusionless civilian transformation

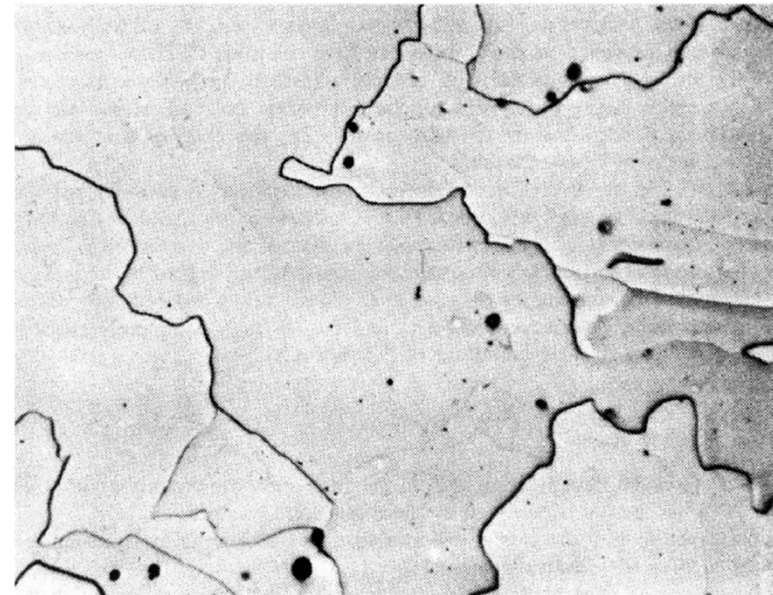
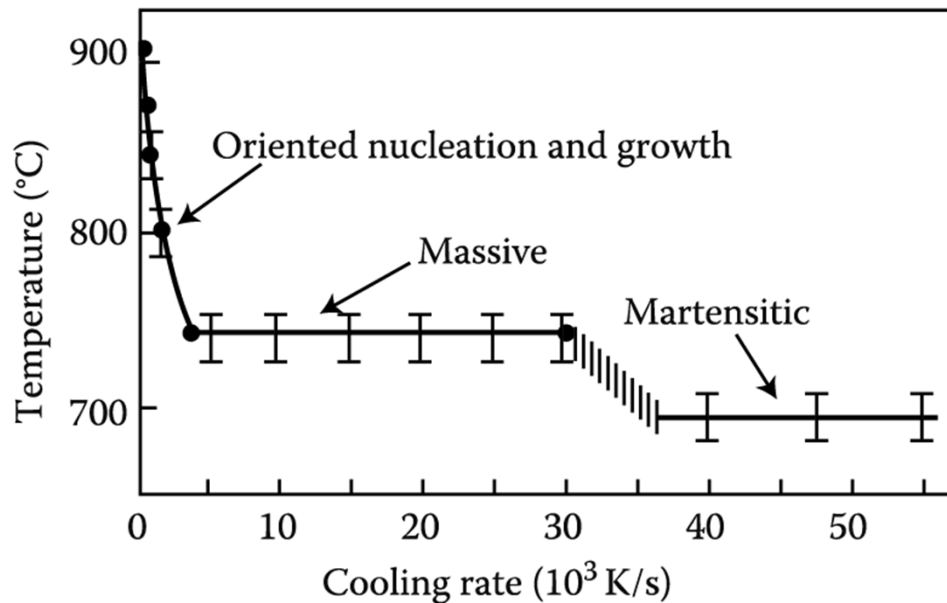


β is sheared into α by the cooperative movement of atoms across a glissile interface
 diffusionless military transformation
Martensite Transformation

Fig. 5.75 A possible CCT diagram for systems showing a massive transformation. Slow cooling (1) produces equiaxed α . Widmanstätten morphologies result from faster cooling (2). Moderately rapid quenching (3) produces the massive transformation, while the highest quench rate (4) leads to a martensitic transformation.

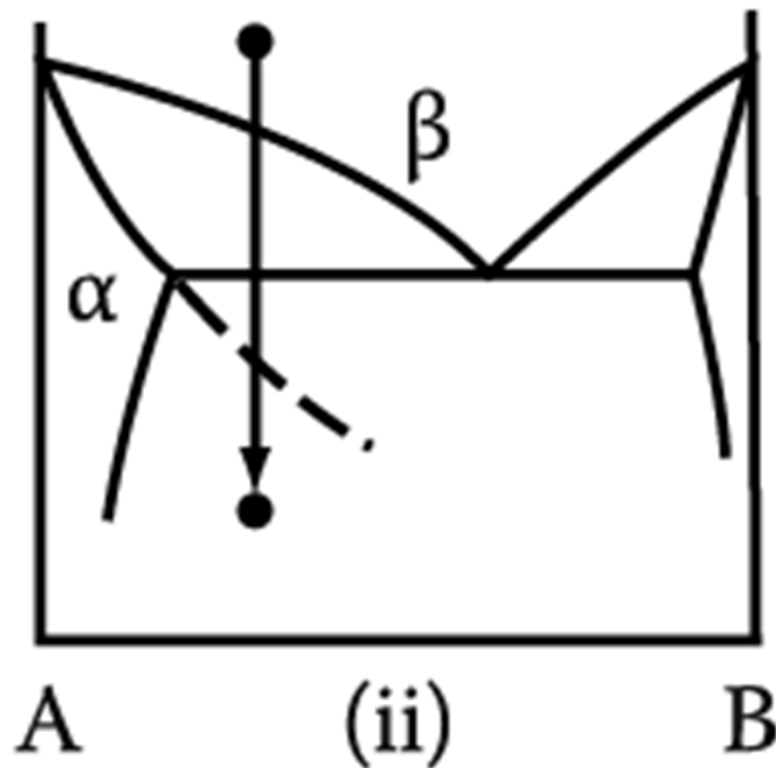
5.9 Massive Transformation: $\gamma \rightarrow \alpha$ transformation in iron and its alloy

Effect of Cooling Rate on the Transformation Temperature at which transformation starts in pure iron



Massive α in an Fe-0.002wt%C
Quenched into iced brine from 1000 °C
: characteristically irregular α/α GBs.

5.9 Massive Transformation



Metastable phases can also form massively.

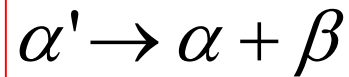
It is not even necessary for the transformation product to be a single phase: **two phases, at least one of which must be metastable**, can form simultaneously provided they have the same composition as the parent phase.

5.10 & 5.11 skip

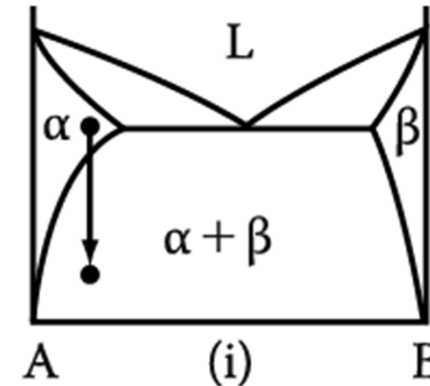
5. Diffusion Transformations in solid

: diffusional nucleation & growth

(a) Precipitation



Metastable supersaturated
Solid solution



Homogeneous Nucleation

$$\Delta G = -V\Delta G_V + A\gamma + V\Delta G_S$$

Heterogeneous Nucleation

$$\Delta G_{het} = -V(\Delta G_V - \Delta G_S) + A\gamma - \Delta G_d$$

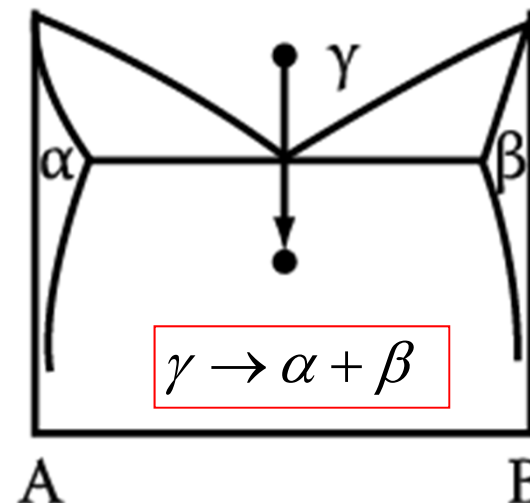
$$N_{hom} = \omega C_0 \exp\left(-\frac{\Delta G_m}{kT}\right) \exp\left(-\frac{\Delta G^*}{kT}\right)$$

→ suitable nucleation sites ~ nonequilibrium defects
(creation of nucleus ~ destruction of a defect (- ΔG_d))

(b) Eutectoid Transformation

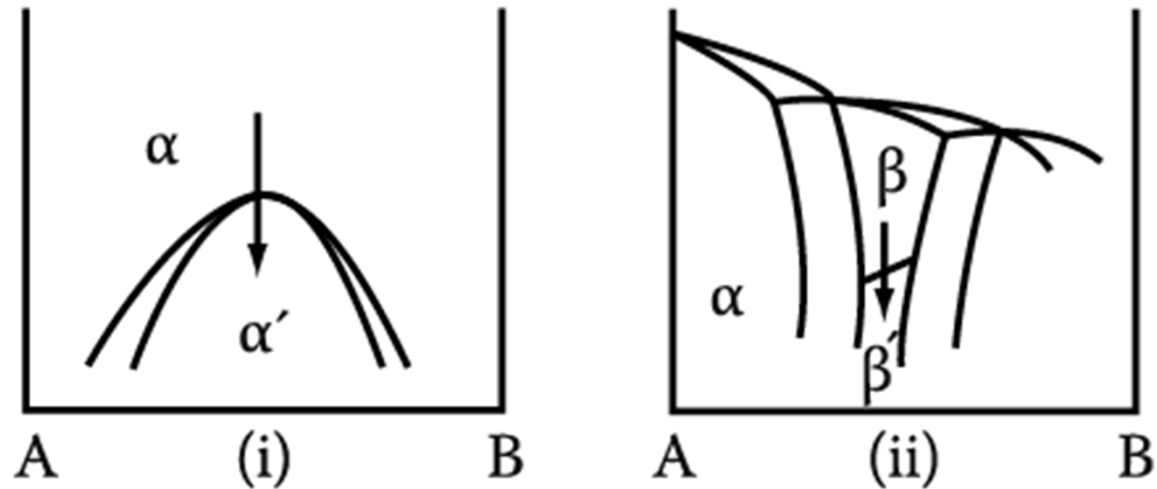
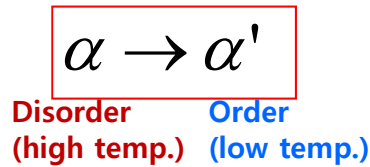
Composition of product phases
differs from that of a parent phase.
→ **long-range diffusion**

Which transformation proceeds
by short-range diffusion?



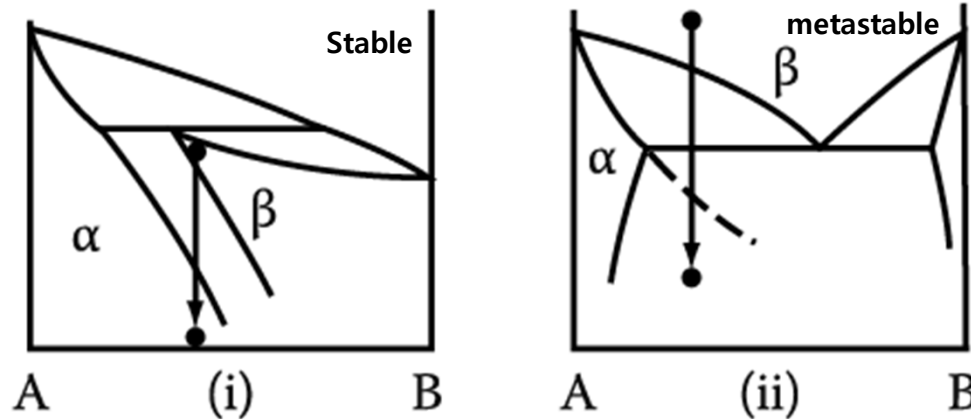
5. Diffusion Transformations in solid

(c) Order-Disorder Transformation

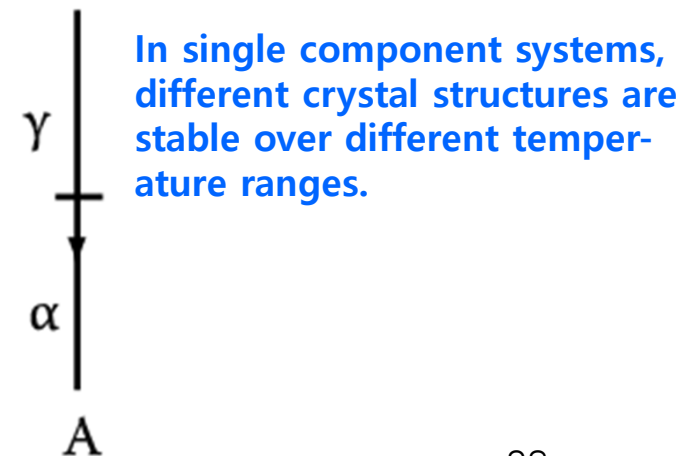


(d) Massive Transformation

: The original phase decomposes into one or more new phases which have the same composition as the parent phase, but different crystal structures.



(e) Polymorphic Transformation



*** Homework 5 : Exercises 5 (pages 379-381)
until 16th December (before exam)**

Good Luck!!

Contents in Phase Transformation

Background
to understand
phase
transformation

(Ch1) Thermodynamics and Phase Diagrams

(Ch2) Diffusion: Kinetics

(Ch3) Crystal Interface and Microstructure

Representative
Phase
transformation

(Ch4) Solidification: Liquid \rightarrow Solid

(Ch5) Diffusional Transformations in Solid: Solid \rightarrow Solid

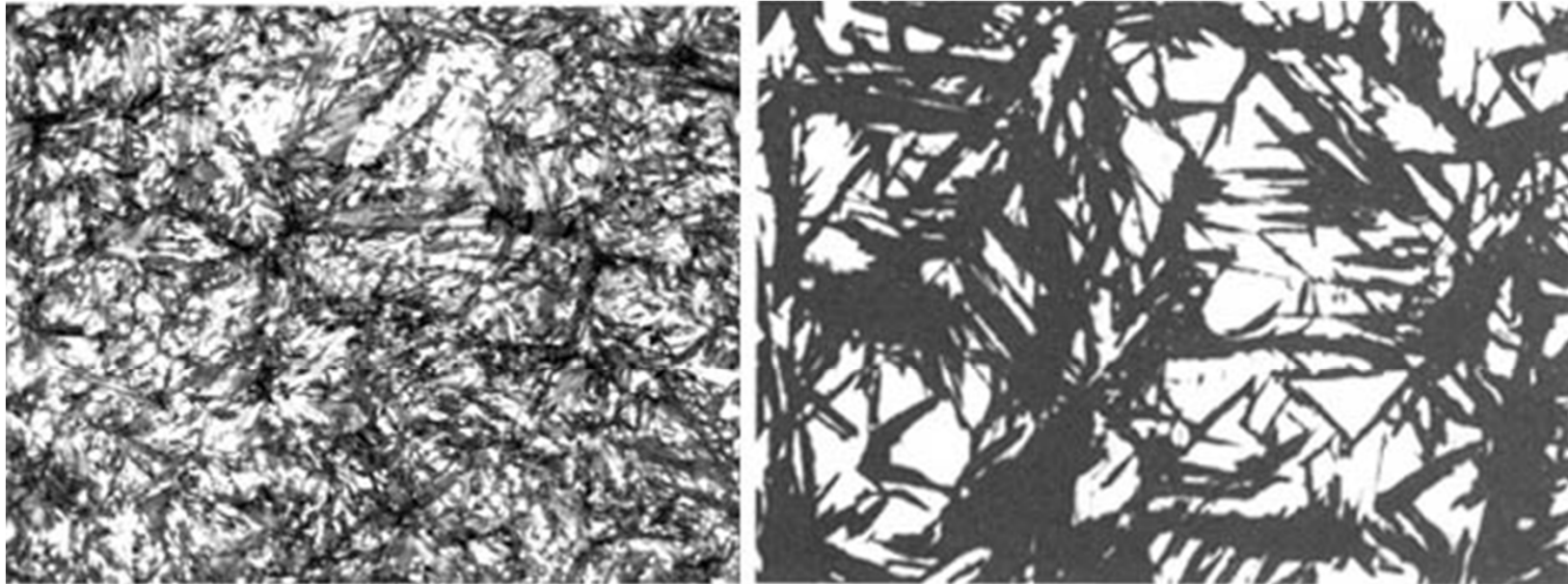
(Ch6) Diffusionless Transformations: Solid \rightarrow Solid

One of the most important technological processes is the hardening of steel by quenching.

Chapter 6 Diffusionless Transformation

Individual atomic movements are less than one interatomic spacing.

→ **Martensite Transformation**



($\gamma \rightarrow \alpha$) Martensite with some retained austenite

"Needle like" Structure of martensite

Supersaturated solid solution of carbon in α -Fe

Named for the German metallurgist **Adolph Martens**, Martensite is **the hardened phase of steel** that is obtained by cooling Austenite fast enough to **trap carbon atoms within the cubic iron matrix distorting it into a body centered tetragonal structure**. Now, martensite is used in physical metallurgy to describe any diffusionless trans. product.

Military Transformations

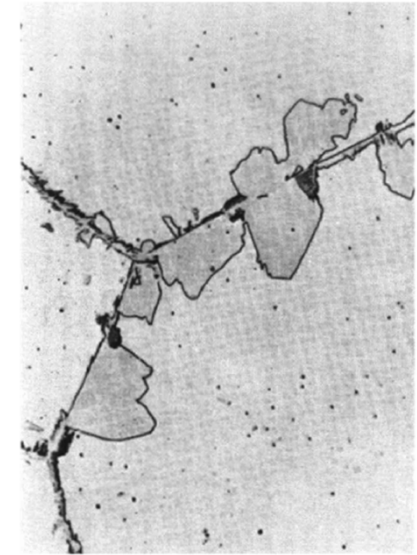
- What is a martensitic transformation?

Most phase transformations studied in this course have been diffusional transformations where long range diffusion is required for the (nucleation and) growth of the new phase(s).

- There is a whole other class of *military transformations* which are *diffusionless transformations* in which the atoms move only short distances (**less than one interatomic spacing**) in order to join the new phase.
- These transformations are *also* subject to the constraints of nucleation and growth. They are (almost invariably) associated with *allotropic transformations* (동소변태).

Massive vs. Martensitic Transformations

- There are two basic types of diffusionless transformations.
- One is the **massive transformation**. In this type, a diffusionless transformation takes place ① without a definite orientation relationship. The interphase boundary (between parent and product phases) migrates so as to allow the new phase to grow. It is, however, a ② civilian transformation because the atoms move individually.
- The other is the **martensitic transformation**. In this type, the change in phase involves a ① definite orientation relationship because the atoms have to ② move in a coordinated manner. There is always a ③ change in shape which means that there is a strain associated with the transformation. The strain is a general one, meaning that all six (independent) coefficients can be different.



Classification of Transformations

	Civilian	Military
Diffusion Required	Precipitation, Spinodal Decomposition	?
Diffusionless	Massive Transformations	Martensitic Transformations

Microstructure of Martensite

- The microstructural characteristics of martensite are:
 - the product (martensite) phase has a well defined crystallographic relationship with the parent (matrix).
- 1) martensite (designated α') forms as **platelets within grains**.

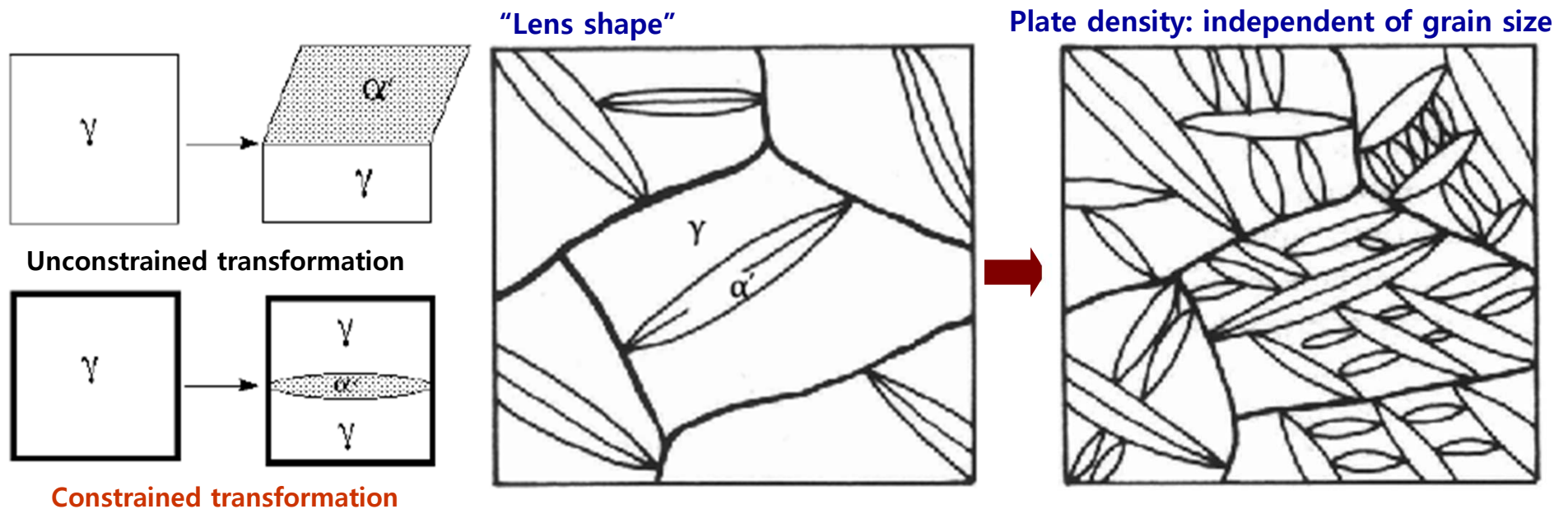


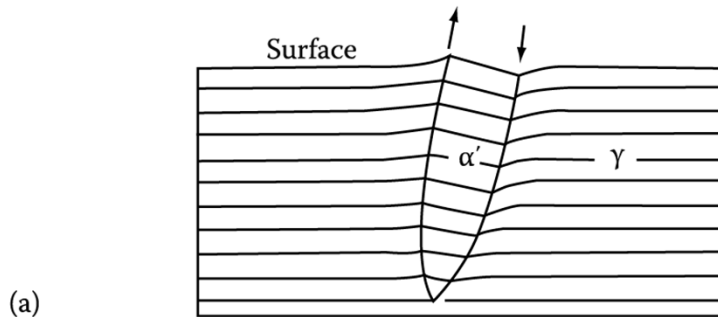
Fig. 6.1 Growth of martensite with increasing cooling below M_s .
→ Martensite formation rarely goes to completion

Microstructure of Martensite

- The microstructural characteristics of martensite are:
 - each platelet is accompanied by a **shape change**.
 - the shape change appears to be a **simple shear parallel to a habit plane** (the common, coherent plane between the phases) and a **uniaxial expansion (dilatation) normal to the habit plane**.

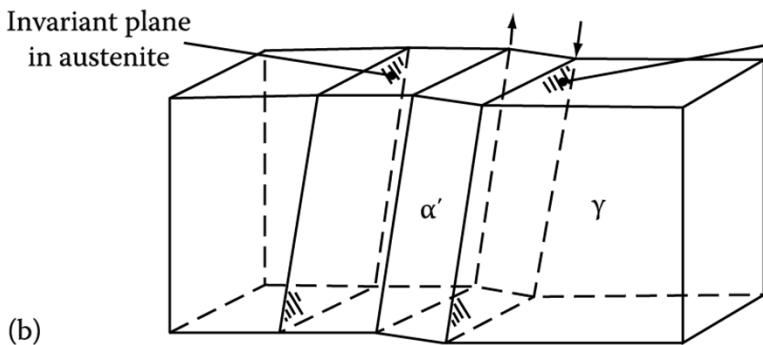
strain associated with the transformation

Polished surface_elastic deformation or tilting
→ but, remain continuous after the transformation



Intersection of the lenses with the surface of the specimen does not result in any discontinuity.

A fully grown plate spanning a whole grain $\sim 10^{-7}$ sec
→ v of α'/γ interface \propto speed of sound in solid



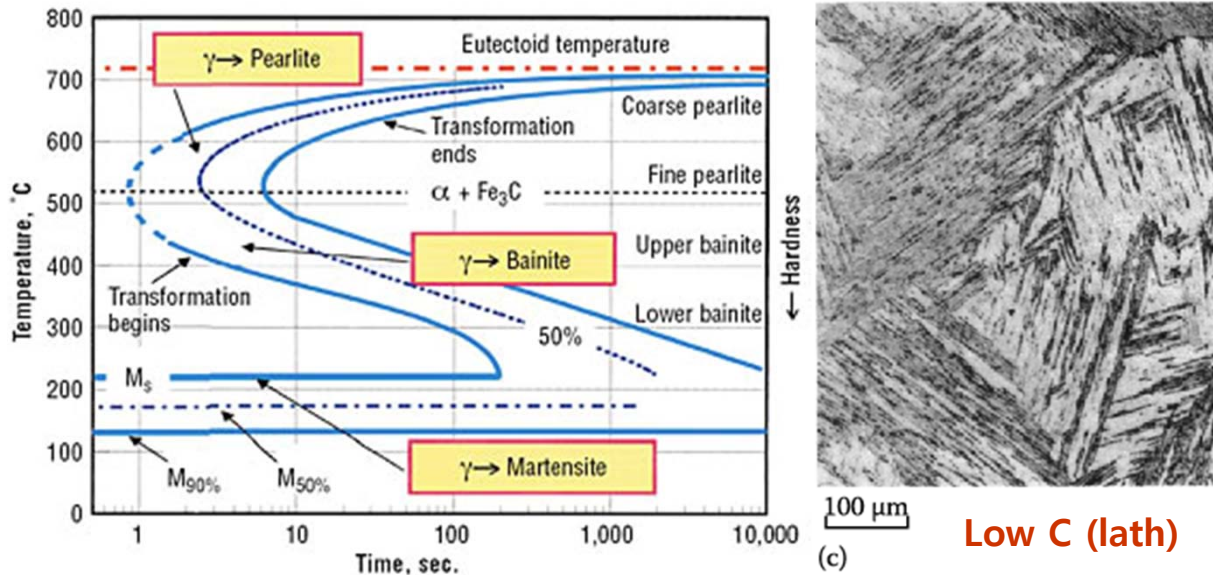
Martensite habit plane

: difficult process to study M nucleation and growth experimentally

Fig. 6.2 Illustrating how a martensite plate remains macroscopically coherent with the surrounding austenite and even the surface it intersects.

Microstructures

M_f temperature (M finish) corresponds to that temperature
 Below which further cooling does not increase the amount of M.
 → 10-15% retained γ : common feature of higher C content alloys



(d) Medium C (plate)



(e) Fe-Ni (plate, some isothermal growth)

Fig. 6.1 (c-e) Different martensite morphologies in iron alloys

Control of Mechanical Properties By Proper Heat Treatment in Iron-Carbon Alloy



Martensite

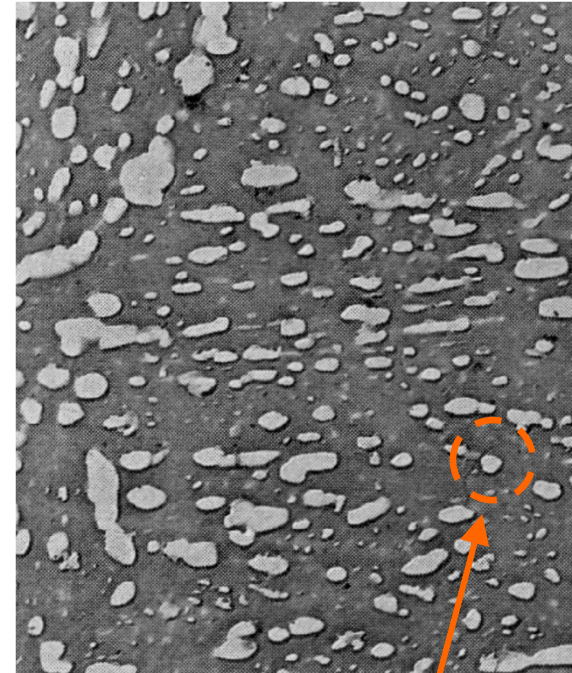
Tip of needle shape grain

Nucleation site of fracture

Brittle



Proper
heat treatment
(tempering)



Tempered martensite

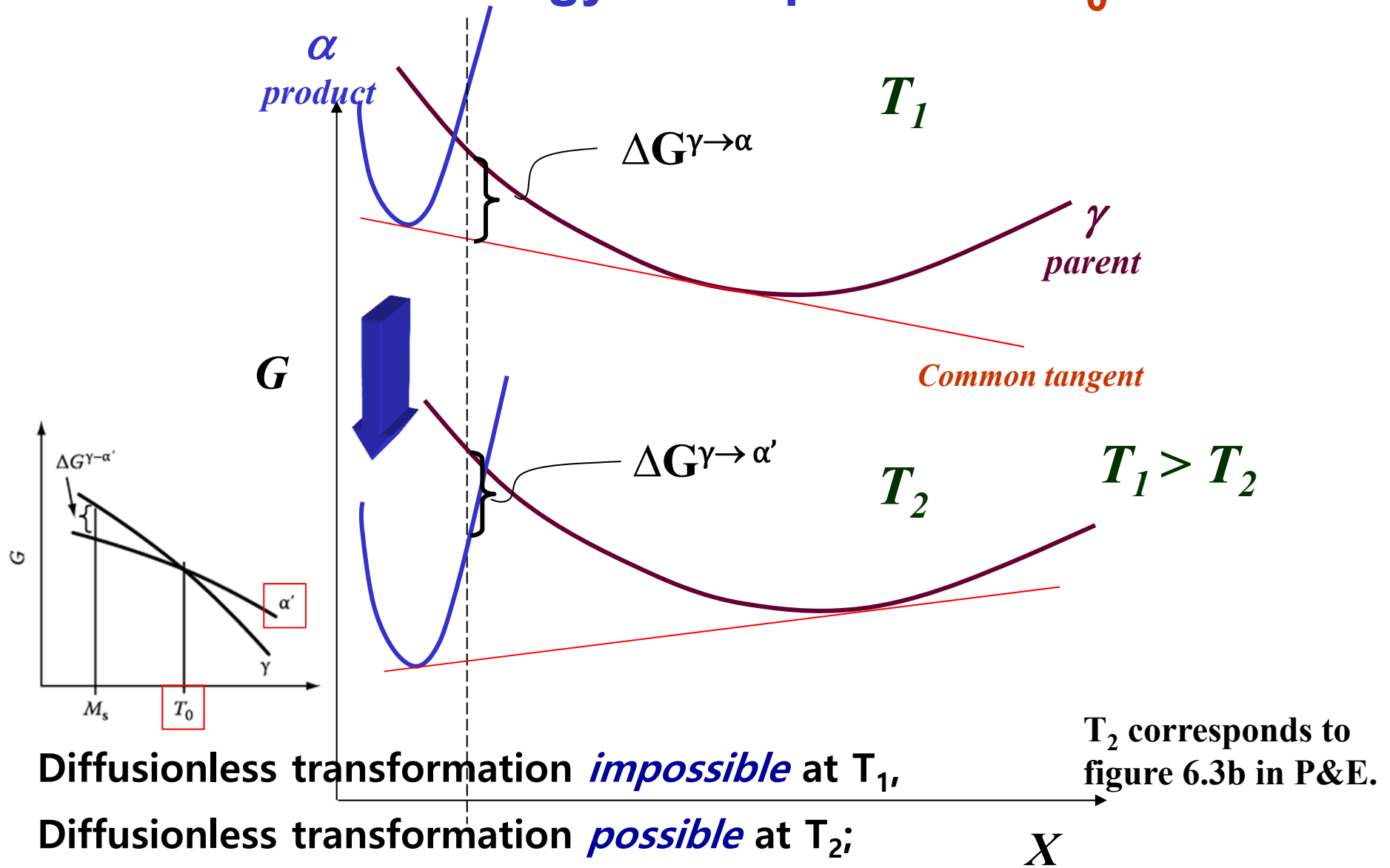
Very small & spherical shape grain

Good strength, ductility, toughness

Driving Forces

- These transformations require **larger driving forces** than for diffusional transformations. (= large undercooling, ΔT)
- Why? In order for a transformation to occur without long range diffusion, it must take place **without a change in composition**.
- This leads to the so-called **T_0 concept**, which is the temperature at which the new phase can appear with **a net decrease in free energy at the same composition as the parent (matrix) phase**.
- As the following diagram demonstrates, the temperature, T_0 , at which segregation-less transformation becomes possible (i.e. a decrease in free energy would occur), is always less than the liquidus temperature.

Free Energy - Composition: T_0



" T_0 " is defined by no difference in free energy between the phases, $\Delta G=0$.

Driving Force Estimation

- The driving force for a martensitic transformation can be estimated in exactly the same way as for other transformations such as solidification.
- Provided that an enthalpy (latent heat of transformation) is known for the transformation, the driving force can be estimated as proportional to **the latent heat** and **the undercooling below T_0** .

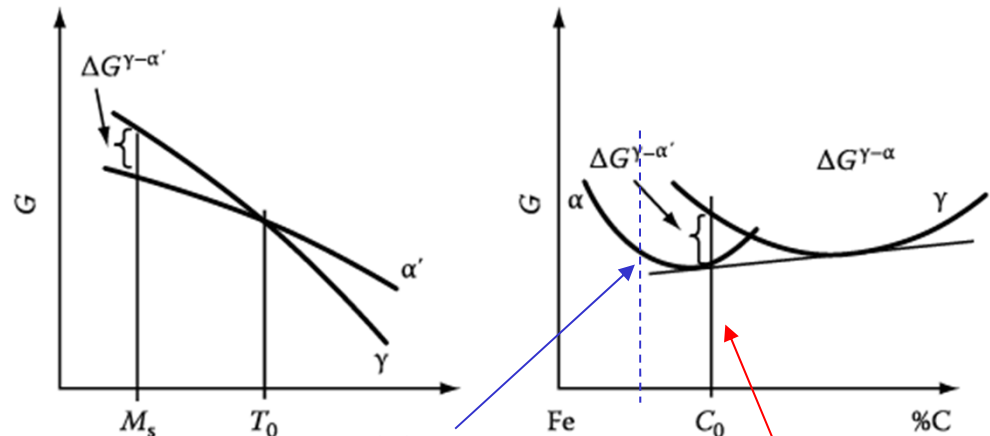
$$\Delta G = \frac{L\Delta T}{T_m} \Rightarrow \Delta G^{\gamma \rightarrow \alpha'} = \Delta H^{\gamma \rightarrow \alpha'} \Delta T / T_0 = \Delta H^{\gamma \rightarrow \alpha'} \frac{(T_0 - M_s)}{T_0}$$

Alloy	$\Delta H^{\gamma \rightarrow \alpha'}$ (J mol ⁻¹)	$T_0 - M_s$ (K)	$-\Delta G^{\gamma \rightarrow \alpha'}$ (J mol ⁻¹)
Ti-Ni	1550	20	92
Cu-Al	170-270	20-60	19.3 ± 7.6
Au-Cd	290	10	11.8
Fe-Ni 28%	1930	140	840
Fe-C			1260
Fe-Pt 24%	340	10	17
Ordered	* Large differences in $\Delta G^{\gamma \rightarrow \alpha'}$ btw disordered and ordered alloys (a relatively small ΔT)		
Fe-Pt	2390	~150	~1260
Disordered			

Source: From Guénin, G., PhD thesis, Polytechnical Institute of Lyon, 1979.

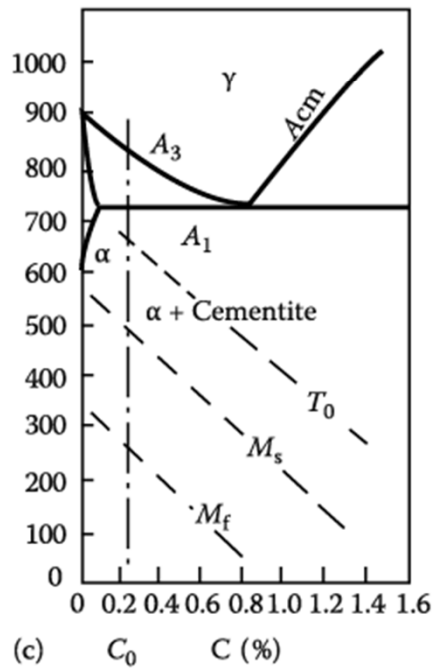
Table 6.1. Comparisons of Calorimetric Measurements of Enthalpy and Undercooling in some M alloys

Various ways of showing the martensite transformation

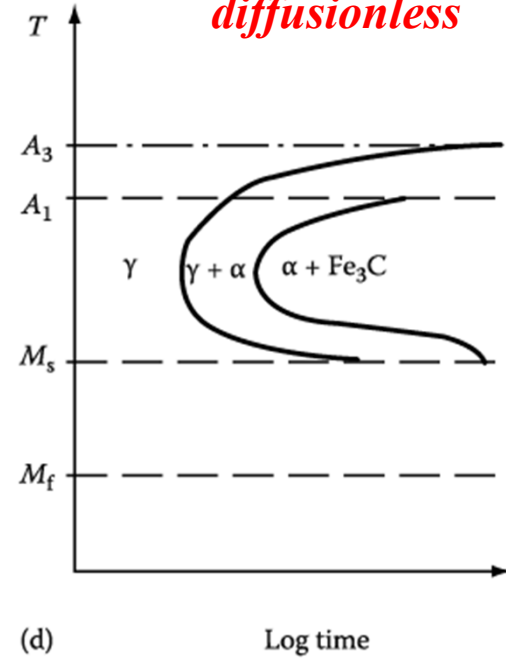


(a) G-T diagram *equilibrium* (b) G-X diagram for C_0 at M_s

diffusionless



(c) Fe-C phase diagram
Variation of $T_0/M_s/M_f$



(d) TTT diagram
for alloy C_0 in (c)

Note that the M_s line is horizontal in the TTT diagram; also, the M_f line.

Some retained austenite can be left even below M_f . In particular, as much as 10%-15% retained austenite is a common feature of especially the higher C content alloys such as those used for ball bearing steels.